Formulation Development (NE)

Part A: Experimental

Chapter 5

5.1 Materials and Equipments

5.1.1 Materials

Dabigatran Etexilate (DE) and Nisoldipine (NISO) were received as gift samples from Alembic Research Centre, Vadodara, India. Peceol, Labrasol, Lauroglycol 90, Capryol 90, Transcutol HP, Lauroglycol FCC were obtained as gift samples from Gattefosse India Private Limited, Mumbai, India. Capmul MCM C8, Capmul MCM, Captex 500, Capmul PG8 were obtained from Abitec, USA. Cremophor EL, Cremophor RH40 were obtained as gift samples from BASF India Ltd., Mumbai, India. All other chemicals and reagents used were of analytical grade.

5.1.2 Equipments

Following is the list of equipments and instruments used for the preparation of NE for DE and NISO.

Table 5.1.1: List of Equipments and Instruments

Name of equipment/ Instrument	Model	Make
Magnetic stirrer	1MLH	Remi Motors, India
High speed homogenizer (Digital Ultra-Turrax)	T-25	IKA®, India
Bath Sonicator	DB-3135	Insref
Probe sonicator	LABSONIC®M	Sartorius Ltd, India
High Pressure Homogenizer	Emulsiflex C5	Avestin, Canada
USP dissolution apparatus	TDT-06P	Labindia, India
pH meter	PICO+	Lab. India, India
Centrifuge	CPR-30	Remi, India
UV-visible double beam spectrophotometer	UV-1800	Shimadzu, Japan
Electronic weighing balance	ELB300	Shimadzu, Japan
Zeta sizer	Nano ZS	Malvern Instruments, UK
Stability chamber	Tanco-PLT 258	S.R Lab Instruments, India
Conductometer	CM-180	ELICO, India

5.2. Fabrication of Nanoemulsion (NE)

5.2.1. Selection of oil phase

Based on results of solubility studies carried out in chapter 4 Part A- section 4.3, Capmul MCM C8 and Peceol were selected as oil phase for the formulation of DE NE and NISO NE respectively.

5.2.2. Selection of S_{mix} system

Based on results of emulsification test and pseudo ternary phase diagrams (Chapter 4 Part B, section 4.7), S_{mix} system consisting of Cremophor EL as surfactant and Transcutol HP as cosurfactant in ratio of 2:1 and 1:1 were selected for DE NE and NISO NE respectively.

5.2.3. Procedure for fabrication of NE

NE was prepared in two stages- preparation of pre-emulsion followed by fine nanoemulsion.

DE-NE: For preparation of oil phase, the required quantity of lipophilic surfactant (Cremophor EL) and drug (DE) were dissolved in oil (Capmul MCM C8) by continuous stirring for 5 min using magnetic stirrer (Remi, India) followed by bath sonication for 1 min. The aqueous phase was prepared by dissolving hydrophilic surfactant (Transcutol HP) in required quantity of distilled water under stirring on magnetic stirrer for 5 min. To prepare pre-emulsion, the oil phase was added drop wise to the aqueous phase using Ultra-turrax at 10000 rpm for 10 min.

Oil in water nanoemulsion loaded with DE was then prepared by high energy emulsification technique by passing through high pressure homogenizer at 10000 psi pressure for 3 cycles. The vessel used to collect homogenized nanoemulsion was kept in ice-water bath to avoid overheating during run. The o/w nanoemulsion thus formed was transferred to clean transparent glass vial, sealed and used for further evaluation. The process and formulation parameters were optimized by full factorial design.

NISO-NE: Pre-emulsion was prepared in similar manner as DE NE with Peceol as oil and NISO as drug. The pre- emulsion was then ultra-sonicated using probe sonication for 9 min at 60% amplitude and 0.6 duty cycles to obtain the nanoemulsion. The o/w nanoemulsion thus formed was transferred to clean amber coloured glass vial, sealed and subjected to characterization. The process and formulation parameters were optimized by full factorial design.

Cleaning of Equipments: After completion of process, the ultra turrax, probe sonicator and HPH assembly were rinsed by alternate cycles of water and methanol to remove any remnants of material, if any.

5.3. Optimization of formulation components for the preparation of pre-emulsion using high speed homogenizer

S_{mix} concentrations of 10% w/v, 15 % w/v and 20% w/v were tried for both DE and NISO NE. The preparations were evaluated on the basis of physical stability of NE (phase separation and appearance) and globule size over a period of 15 days. The oil concentration was kept at 10 % w/v for both the NE. Water concentration was taken as 73% w/v and 69 % w/v for DE NE and NISO NE respectively. Phase separation and changes in appearance of prepared NE were checked through visual observations and the globule size was determined by Zetasizer (NanoZS, Malvern Instruments, UK).

5.4. Optimization of process parameters for the preparation of pre-emulsion using high speed homogenizer (ultra turrax)

Effect of homogenization speed and homogenization time were studied on GS and PDI for both the formulations. Parameters are recorded as shown in table 5.4.1.

Table 5.4.1. Parameter range to study the effect of homogenization speed and homogenization time

Parameter	Range	Response studied
Homogenization speed	8000,10000,12000 and 14000 RPM	Globule size and PDI
Homogenization time	5, 10 and 15 min	

5.5. Optimization of DE NE and NISO NE by full factorial design

Factorial design is used to study the effect of independent variables on the dependent variables of any formulation. Based on the principle of design of experiments, factorial design is employed to evaluate the effect of two independent factors [1]. The regression equation for the response is calculated using the equation below:

$$Y=b_0+ b_1X_1+ b_2b_2+ b_3X_{12}+ b_4X_{22}+ b_5X_1X_2 \quad \text{.....Eqn. 5.5.1}$$

In this mathematical approach, each experimental response (Y) can be represented by a quadratic equation of the response surface. Y is the measured response and b is the estimated coefficient for the factor X. The coefficients are corresponding to linear effects (X_1 and X_2), interaction (X_1X_2) and the quadratic effects (X_{12} and X_{22}) [2].

DE NE: Nanoemulsion optimization was done using three level full two factor full factorial design to study the influence of the effect of independent variables [Homogenization Pressure (psi) (X_1) and No. of homogenization cycles (X_2)] on critical dependent variables [globule Size (Y_1) and PDI(Y_2)]. The design layout (Table 5.5.1) was set based on the preliminary experiments.

Table 5.5.1.: Design layout of 3^2 full factorial design for DE NE

Variables (Factors)	Levels		
	−1	0	1
X1: Homogenization Pressure (psi)	5000	10000	15000
X2: No. of homogenization cycles	2	3	4
Responses	Constraints		
Y_1= Globule size (nm)	Minimize		
Y_2= PDI	Minimize		

NISO NE: Optimization was done using three level two factor factorial design to study influence of the independent variables [Probe sonication time (min) (X_1) and Amplitude (%) (X_2)] on critical dependent variables [globule Size (Y_1) and PDI(Y_2)]. The design layout (Table 5.5.2) was set based on the preliminary experiments.

Table 5.5.2: Design layout of 3^2 full factorial design for NISO NE

Variables (Factors)	Levels		
	−1	0	1
X1: Probe sonication time (min)	6	9	12
X2: Amplitude (%)	40	60	80
Responses	Constraints		
Y1= Globule size (nm)	Minimize		
Y2= PDI	Minimize		

The three level two factor full factorial design comprised of 13 runs and 9 runs for DE NE and NISO NE respectively. Both the designs allowed the fitting of Quadratic model on two responses for process optimization in preparation of DE NE and NISO NE with minimum Globule size and PDI. Contour plots and response surface plots were also generated. Check point batch suggested by software was prepared and the percentage relative error of each response was calculated using the following equation in order to judge the validity of the model.

$$\% \text{ Relative Error} = \frac{\text{Predicted value} - \text{Experimental value}}{\text{Predicted value}} * 100 \qquad \text{.....Eqn 5.5.2}$$

Desirability function

For simultaneous optimization of response variables (GS and PDI), a multi-response optimization technique also known as desirability function was applied and total desirability was calculated using Design Expert software (version 7.0.3, Suite, Minneapolis, USA) for both the formulations. The desirability between 0 and 1 represents the closeness of a response to its ideal value [3].

Statistical analysis

The results for both the formulations were presented as mean ± standard error of the mean. The experimental data were validated by ANOVA, regression coefficient, lack of fit test and $p < 0.05$ was considered as significant.

5.6. Characterization of optimized batch of DE NE and NISO NE

5.6.1. Globule size, poly dispersity index (PDI)

Globule size analysis was executed by photon correlation spectroscopy (PCS) with Zetasizer using dynamic light scattering (Malvern, Nano ZS, UK). Photon correlation spectroscopy yields mean particle size and polydispersity Index (PDI). PDI represents the width and particle size distribution of the sample. Globule Size, PDI of the DE NE and NISO NE formulations were determined after dilution (1:250) with distilled water. [4]. All studies were performed in triplicate.

5.6.2. Measurement of Zeta potential

Zeta potential was measured using Zetasizer (NanoZS, Malvern Instruments, UK). For measurement of zeta potential, the diluted samples of DE NE and NISO NE were filtered

through 0.22 µm Millipore filters and placed in a disposable cuvette of the Zetasizer. The electrophoretic mobility (mm/s) was converted to zeta potential by in-built software using Helmholtz–Smoluchowski equation [5]. All studies were performed in triplicate.

5.6.3. Drug content

Optimized batch of DE and NISO NE equivalent to 20mg of DE and 10 mg of NISO were dispersed into appropriate quantity of methanol, stirred sufficiently to dissolve the drug, and centrifuged at 3000rpm for 10min [6]. The supernatants were duly diluted and analyzed spectrophotometrically (UV-1800 Shimadzu, Japan) at 315nm for DE and at 236 nm for NISO.

5.6.4. pH

The pH of DE NE and NISO NE were measured by using digital pH meter (Systronics 335, India), standardized using pH 4 and pH 7 standard buffers before use [7].

5.6.5. Morphological examination using Transmission Electron Microscopy (TEM)

The morphology of the oil globules of DE NE and NISO NE were visualized using TEM. A drop of nanoemulsion formed after dilution (100-fold dilution in distilled water) of the optimized NE was placed on a piece of parafilm. A carbon coated grid (3mm, 300#) was placed on top of the drop and left for 1 min. Excess fluid was removed by using filter paper. Negative staining was then performed by placing the grid on a drop of 2% phosphotungsten acid (PTA) for 1 min. The grid was examined under a transmission electron microscope (Tecnai 20, 200KV, Phillips, Netherland) [4].

5.6.6. Conductivity

Conductivity measurements were carried out to demonstrate the effect of water dilution on the NE structure. Conductivity of DE NE and NISO NE were measured by Conductometer (CM-180 ELICO, India) which was calibrated using 0.001 M KCl prior to use. Distilled water was added drop wise to the NE and the change in conductivity with increase in the amount of water was recorded [8].

5.6.7. Viscosity

The viscosity of the optimized batch of DE NE and NISO NE were determined employing Brookfield viscometer (DV-III+ Rheometer, Brookfield, USA) using cone and plate at 10 rpm speed and 25°C in triplicate.

5.6.8. Thermodynamic stability assessment

Thermodynamic stability assessment was carried out same as procedure explained in section 4.4.2.

5.6.9. Fourier transform infrared (FTIR) spectroscopy

The FTIR spectra of optimized formulation was compared with individual spectra of both the pure drugs and placebo mix of excipients used in fabrication of DE NE and NISO NE. Procedure as described in section 4.2.1.2 was followed.

5.6.10. Drug release studies

Drug release studies including i*n vitro* dissolution study, i*n vitro* diffusion study and e*x vivo* release study were carried out same as procedure described in section 4.4.11.

5.7. Stability study

The optimized batches of DE NE and NISO NE were packed into sealed transparent and amber coloured glass bottles respectively [9] and subjected to accelerated and long term stability testing according to the ICH guidelines for zones III and IV (ICH Q1A (R2), 2003) at 40 ± 2^0C/75 ± 5% RH (for 0,1, 2, 3 and 6 months) and 25 ± 2^0C/60 ± 5% RH (for 0, 1, 3 and 6 months) conditions. The samples were withdrawn periodically and evaluated for different physicochemical parameters like globule size and drug content. Stability samples were also observed visually for creaming, cracking or phase separation.

References

1. B.P. Sahu and M.K. Das, Optimization of felodipine nanosuspensions using full factorial design. International Journal of Pharm. Tech Research, 2013. 5(2): p. 553-561.
2. K.K. Sawant, M.H. Patel, and K. Patel, Cefdinir nanosuspension for improved oral bioavailability by media milling technique: formulation, characterization and in vitro–in vivo evaluations. Drug development and industrial pharmacy, 2016. 42(5): p. 758-768.
3. K.K. Sawant, V.P. Mundada, and V.J. Patel, Development and Optimization of w/o/w Multiple Emulsion of Lisinopril Dihydrate Using Plackett Burman and Box-Behnken Designs. J Nanomed Nanotechnol, 2017. 8(1): p. 422.
4. S. Gupta, S. Chavhan, and K.K. Sawant, Self-nanoemulsifying drug delivery system for adefovir dipivoxil: design, characterization, in vitro and ex vivo evaluation. Colloids and Surfaces A: Physicochemical and Engineering Aspects, 2011. 392(1): p. 145-155.
5. A. Kumar and K.K. Sawant, Application of multiple regression analysis in optimization of anastrozole-loaded PLGA nanoparticles. J Microencapsul, 2014. 31(2): p. 105-14.
6. S.T. Prajapati, H.A. Joshi, and C.N. Patel, Preparation and characterization of self-microemulsifying drug delivery system of olmesartan medoxomil for bioavailability improvement. Journal of pharmaceutics, 2012. 2013.
7. S.P. Acharya, K. Pundarikakshudu, A. Panchal, and A. Lalwani, Preparation and evaluation of transnasal microemulsion of carbamazepine. Asian Journal of Pharmaceutical Sciences, 2013. 8(1): p. 64-70.
8. S.S. Solanki, B. Sarkar, and R.K. Dhanwani, Microemulsion Drug Delivery System: For Bioavailability Enhancement of Ampelopsin. ISRN Pharmaceutics, 2012. 2012: p. 108164.
9. Y.S. Elnaggar, M.A. El-Massik, and O.Y. Abdallah, Self-nanoemulsifying drug delivery systems of tamoxifen citrate: design and optimization. International journal of pharmaceutics, 2009. 380(1): p. 133-141.

Formulation Development (NE)

Part B: Result & Discussion

Chapter 5

Homogenization is one of the most frequently used techniques for preparing emulsions. The nanoemulsions were produced by a 2-stage homogenization procedure as the pre-emulsion obtained from the first stage (high speed homogenization) had to be further broken in the second stage (under high pressure and probe sonication for DE and NISO NE respectively).

It is well known that process parameters such as the homogenization pressure, number of homogenization cycles, probe sonication time and probe sonication amplitude can affect the physical characteristics and stability of the emulsions. Therefore, optimization studies were conducted with the aim of finding the optimal conditions and to investigate the effect of these parameters on characteristics of NEs viz globule size, PDI etc. The value of Z-average diameter that is referred to as the harmonic intensity-weighted average hydrodynamic diameter of the emulsions was reported as mean globule size of emulsions. The PDI is a dimensionless measure ranging from 0 to 1. Smaller value of PDI indicates a monodispersed population, while a larger PDI indicates a broader distribution of droplet size [1].

5.8. Optimization of formulation components for the preparation of pre-emulsion using high speed homogenizer

The effect of S_{mix} concentration (10% w/v to 20% w/v) on globule size, phase separation and appearance for both DE and NISO was studied for 15 days and results are as shown in Table 5.8.1. Globule size was not measured for the NE where phase separation was observed.

Table 5.8.1. Effect of S_{mix} system concentration for DE NE and NISO NE

		Day 1		Day 7		Day 15	
Formulations	**S_{mix} Conc. (% w/v)**	**Visual observation**	**Globule Size (nm)**	**Visual observation**	**Globule Size (nm)**	**Visual observation**	**Globule Size (nm)**
DE NE S_{mix} (2:1)	10	Stable but clear	636.48 ± 4.43	Phase separation	--	--	--
	15	Stable and clear	249.89 ± 2.29	Stable and clear	250.22 ± 2.02	Stable and clear	248.85 ± 1.88
	20	Stable and clear	255.54 ± 2.14	Stable and clear	246.67 ± 2.11	Stable and clear	253.74 ± 2.08
NISO NE S_{mix} (1:1)	10	Stable but clear	779.57 ± 4.98	Phase separation	--	--	--
	15	Stable and clear	436.84 ± 3.63	Stable but turbid	888.69 ± 5.12	Phase separation	--
	20	Stable and clear	256.37 ± 2.37	Stable and clear	259.74 ± 2.16	Stable and clear	264.41± 2.13

Influence of Surfactant concentration

From the above results (Table 5.8.1), 15% w/v of S_{mix} concentration for DE NE and 20% w/v of S_{mix} concentration for NISO NE were finalized for the fabrication of respective NE. It was observed that stable and clear DE NE was formed at both 15% w/v and 20% w/v with almost similar globule size but 15% w/v S_{mix} concentration was finalized as it is well known that high concentration of surfactant is toxic to GIT and may cause moderate reversible changes in intestinal wall permeability [2].

The amount of surfactant plays vital role in NE formation. It was observed that as the surfactant concentration increased, globule size was decreased. This might be due to the fact that higher concentration of surfactant provides better coverage of the interface and further reduces interfacial tension to facilitate droplet rupture during homogenization and leads to lower globule size [3]. Moreover, higher proportion of surfactant may provide closely packed interfacial surfactant film, thereby stabilizing the oil droplets. When droplet size decreases from micron to nanoscale, the specific surface area increases immensely. The globule size was markedly high at 10 % w/v concentration which might be due to the fact that at lower surfactant concentration, the amount of surfactant available was not able to cover the nano-droplets which led to their coalescence, in turn increased the particle size and caused phase separation [4].

5.9. Optimization of process parameters for the preparation of DE and NISO pre-emulsion using high speed homogenizer (ultra turrax)

The effect of homogenization speed (8000, 10000, 12000 and 14000 RPM) and homogenization time (5, 10 and 15 min) on globule size and PDI of the pre-emulsion for both DE and NISO was studied and results are shown in Table 5.9.1 and Table 5.9.2 respectively.

Influence of homogenization speed

It was observed from the results that homogenization speed had significant effect on globule size of DE and NISO NE. When the homogenization speed increased from 8000 to 10000 rpm, globule size of the nanoemulsion decreased. As the speed of stirring is increased, it may lead to breakup of the bigger oil globules into many fine oil droplets but further increase would lead to increase in globule size [5]. However, additional increase in homogenization speed from 10000 to 12000 led to increase in globule size. This might be due to the fact that at higher homogenization speed, the flow behavior changes from Newtonian to shear thickening which could lead to coalescence [6]. Turbidity occurred at higher speed i.e. 14000

RPM due to the coalescence of globules in both the formulations. In both cases, polydispersity index (PDI) was more than 0.250 indicating non-uniform distribution. Thus, 10000 RPM of homogenization speed was considered suitable for obtaining pre-emulsion with desired globule size and uniform PDI for DE and NISO NE.

Influence of homogenization time

Globule size decreased with increase in time period from 5 to 10 min but further as time increased to 15 min, no significant difference was observed in globule size and PDI increased. High homogenization time may cause instability of colloidal globules due to high input of energy that leads to aggregation of colloidal globules into larger globules. Thus, 10 minutes of homogenization time was considered suitable for obtaining pre-emulsion of DE and NISO NE.

Table 5.9.1. Effect of homogenization speed and homogenization time on globule size and PDI for DE NE pre-emulsion

Sr. No.	Homogenization speed (RPM)	Homogenization Time (min)	Globule size (nm)	PDI
1	8000	5	515.82± 4.2	0.594± 0.03
2	10000		420.51± 5.8	0.499± 0.02
3	12000		499.24± 5.6	0.462± 0.04
4	14000		Turbid	--
5	8000	10	489.73± 4.4	0.397± 0.04
6	10000		288.22± 3.1	0.235± 0.03
7	12000		302.47± 3.9	0.321± 0.05
8	14000		Turbid	--
9	8000	15	491.28± 4.1	0.390± 0.01
10	10000		289.45± 3.2	0.368± 0.08
11	12000		300.76± 3.5	0.317± 0.07
12	14000		Turbid	--

Table 5.9.2. Effect of homogenization speed and homogenization time on globule size and PDI for NISO NE pre-emulsion

Sr. No.	Homogenization speed (RPM)	Homogenization Time (min)	Globule size (nm)	PDI
1	8000	5	505.29±3.9	0.512±0.05
2	10000		443.63±4.4	0.416±0.03
3	12000		490.26±5.2	0.458±0.04
4	14000		Turbid	--
5	8000	10	435.44±4.5	0.418±0.04
6	10000		279.82±3.9	0.238±0.02
7	12000		310.65±4.1	0.333±0.06
8	14000		Turbid	--
9	8000	15	432.33±4.3	0.421±0.07
10	10000		281.47±4.0	0.365±0.04
11	12000		311.31±3.4	0.335±0.03
12	14000		Turbid	--

5.10. Optimization of DE NE and NISO NE by full factorial design

5.10.1. Optimization of DE NE

Homogenization pressure and number of homogenization cycles were taken as independent variables as they significantly affect the globule size and PDI. Effects of homogenization pressure and number of homogenization cycles on responses such as globule size and PDI were optimised using three level two factor full factorial design**.** Thirteen batches of DE NE were prepared varying independent variables and responses were recorded (Table 5.10.1). The GS and PDI values for the 13 batches showed a wide variation from 71.65 to 146.10 nm and 0.109 to 0.486 respectively. Total 13 runs were obtained as 4 centre points per block were selected to make the design more robust. When the results were subjected to data analysis by multiple linear regression followed by ANOVA employing Design Expert® software (Version 8.0.3, Suite, Minneapolis, USA), the model fitting was found to be highly significant for both the response variables ($p < 0.0001$). Both responses were found to have good model fitting with insignificant Lack of Fit indicating aptness of the model for future prognostic purposes. The polynomial equations 5.10.1 and 5.10.2 were generated by the statistical analysis of the results:

$Y_1 = 76.36 - 17.04X_1 - 9.05X_2 - 4.29X_1X_2 + 32.39X_1^2 + 13.73X_2^2$ .....Eqn 5.10.1

$Y_2 = 0.15 - 0.092X_1 - 0.064X_2 - 0.016X_1X_2 + 0.13X_1^2 + 0.077X_2^2$ .....Eqn 5.10.2

Table 5.10.1: Design matrix for 3^2 factorial design for DE NE

Runs	Homogenization Pressure (psi) (X_1)	Homogenization cycle (No.) (X_2)	Globule Size (nm) (Y_1)	PDI (Y_2)
1	5000	3	125.80 ± 3.98	0.398 ± 0.07
2	10000	3	79.99 ± 1.74	0.176 ± 0.06
3	10000	3	74.35 ± 1.63	0.133 ± 0.04
4	10000	2	95.68 ± 2.71	0.295 ± 0.07
5	10000	3	71.65 ± 1.59	0.109 ± 0.04
6	5000	4	132.90 ± 4.99	0.387 ± 0.02
7	15000	2	120.4 ± 3.97	0.353 ± 0.07
8	15000	3	92.14 ± 2.75	0.177 ± 0.04
9	10000	3	77.12 ± 1.69	0.178 ± 0.03
10	15000	4	90.03 ± 2.87	0.191 ± 0.05
11	10000	3	78.23 ± 1.68	0.139 ± 0.02
12	10000	4	84.94 ± 1.84	0.171 ± 0.06
13	5000	2	146.10 ± 4.96	0.486 ± 0.09

All the responses were analysed statistically at 5% level of significance and p value obtained for each response was less than 0.05. All responses were simultaneously fitted to linear, quadratic, special cubic and cubic models by using the Design-Expert software version 7.0. Out of these, quadratic model was found to be significant for both the responses studied. The p-value and t-stat demonstrated the significance of each coefficient for both the responses (Table 5.10.2 and 5.10.3). Lack of fit was not significant for both the responses which signifies good model fitting. The predicted R-Squared for both the responses were in reasonable agreement with the adjusted R-Squared indicating that the selection and model fitting were acceptable (Table 5.10.4).

Table 5.10.2: Results of ANOVA for globule size of DE NE

Source	Sum of Squares	df	Mean square	F Value	p-value prob>F	
Model	7398.66	5	1479.73	122.55	< 0.0001	Significant
X_1	1741.83	1	1741.83	144.25	< 0.0001	
X_2	491.60	1	491.60	40.71	0.0004	
X_1X_2	73.70	1	73.70	6.10	0.0428	
X_1^2	2896.84	1	2896.84	239.91	< 0.0001	
X_2^2	520.35	1	520.35	43.09	0.0003	
Residual	84.52	7	12.07			
Lack of Fit	41.09	3	13.70	1.26	0.3998	Not Significant

Table 5.10.3: Results of ANOVA for PDI of DE NE

Source	Sum of Squares	df	Mean square	F Value	p-value prob>F	
Model	0.18	5	0.035	50.77	< 0.0001	Significant
X_1	0.050	1	0.050	72.92	< 0.0001	
X_2	0.025	1	0.025	35.73	0.006	
X_1X_2	9.923E-004	1	9.923E-004	1.44	0.2699	
X_1^2	0.048	1	0.048	68.77	< 0.0001	
X_2^2	0.016	1	0.016	23.50	0.0019	
Residual	4.840E-003	7	6.914E-004			
Lack of Fit	1.334E-003	3	4.446E-004	0.51	0.6981	Not Significant

Table 5.10.4: Model Statistics for Y1 and Y2 responses for DE NE using 3^2 full factorial design

Response	Model	Model F-value	R-Squared	Adjusted R-Squared	Predicted R-Squared	Lack of Fit p-value	Std. Dev.
Y1	Quadratic	122.55	0.9887	0.9806	0.9358	0.3998	3.47
Y2	Quadratic	50.77	0.9732	0.9540	0.9011	0.6981	0.026

Influence of Homogenization Pressure on globule size and PDI

Homogenization pressure can significantly influence the properties of emulsions as the shear forces and turbulence, both of which are pressure dependent, produced during homogenization can affect the globule size and size distribution [7]. The minimum globule size and PDI observed in this study was 71.65 nm and 0.109 respectively. As shown in Table 5.10.1, increasing the homogenization pressure resulted in significant ($P < 0.05$) decrease in the globule size and PDI. Homogenization pressure when increased from 5000 psi to 10,000 psi, led to decrease in the globule size and PDI. This could be accredited to inertial forces that govern the process at high pressure and break the bigger droplets due to pressure fluctuations from turbulence and led to decrease in GS and PDI [8]. This type of trend can also be seen when the interfacial tension decreases, the emulsifier adsorption rate increases, and the disperse-to-continuous phase viscosity ratio falls within a certain range [9]. However, further increase in pressure from 10,000 psi to 15,000 psi, led to increase in GS and PDI. This might be due to the amplified kinetic energy of the system, resulting in increased particle collision and thus coagulation. The high rate of particle collisions also deform the surfactant film on the particle surface and build up the particle aggregation [10]. Uniformity of globule size distribution is measured by PDI; nanoemulsions are generally referred to as 'monodisperse' if PDI is less than 0.200 [11]. ANOVA results (Table 5.10.3) show that the homogenization pressure significantly ($p<0.05$) affect the PDI values of DE and NISO NE.

Influence of Homogenization cycle on droplet size and PDI

The effect of homogenization cycle on the responses of DE NE are presented in table 5.10.1. As expected, increasing the homogenization cycle resulted in significant decrease ($P < 0.05$) in both the globule size and its PDI. Globule size and PDI were negatively influenced by number of homogenization cycle. After three homogenization cycles, significant decrease in globule size and PDI was observed. However, on subsequent increase in number of cycles from three to four globule size increased, but no further improvement in the size PDI was observed. The in homogeneities during the passage of emulsion through piston might be the reason for the variation in PDI [12]. However, ANOVA results (Table 5.10.3) show that the homogenization cycle significantly ($p<0.05$) affect the PDI values of DE and NISO NE.

Contour plots and response surface analysis

For each response, globule size and PDI, contour plots were established between X_1 and X_2. From the plots, it is clear that the globule size was maximum at the mid value of X_1 and X_2

i.e. homogenization pressure of 10,000 and 3 homogenization cycles (Figure 5.10.1). Lower globule size and higher PDI was observed on the sides of blue zone in the contour plot. Response surface plots show the relationship between these variables even more clearly when plotted between X_1 and X_2 (Figure 5.10.2).

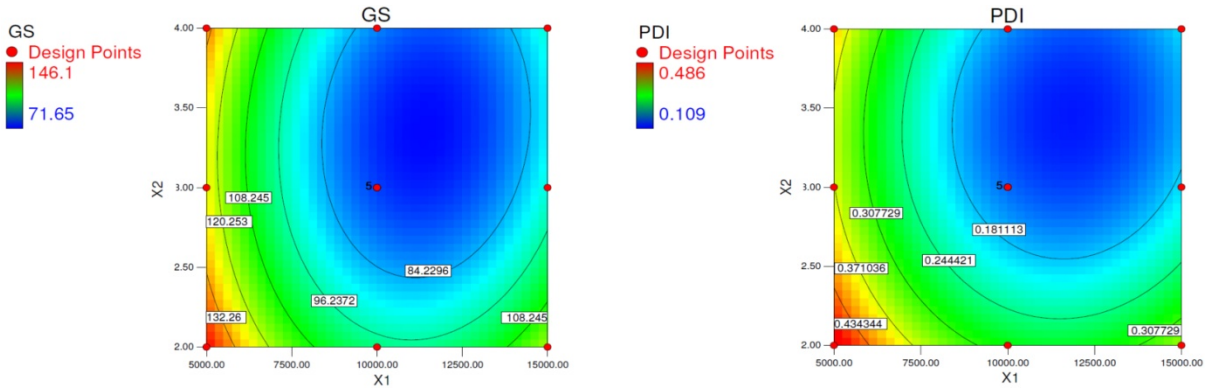

Figure 5.10.1. Contour plots showing effect of independent variables on GS and PDI for DE NE

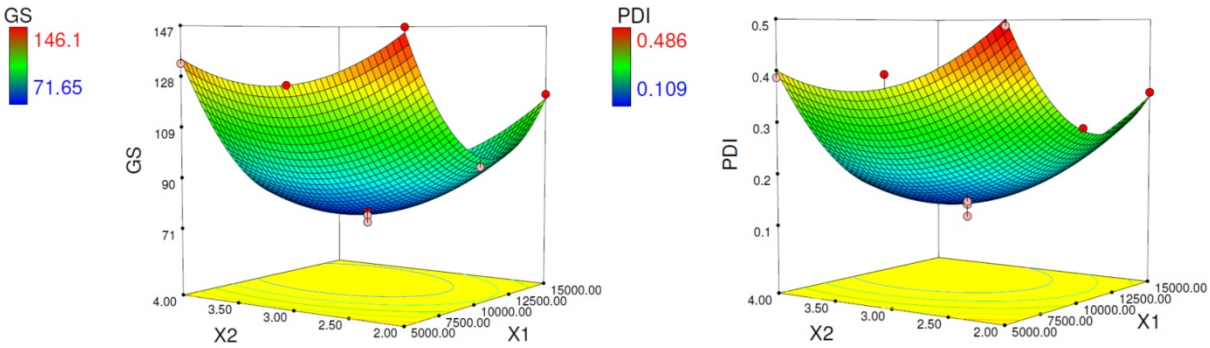

Figure 5.10.2. Response surface plots showing effect of independent variables on GS and PDI for DE NE

Check point analysis/desirability function

Desirability function can be used to validate the selected model. The desirability function is a procedure used to optimize multi response analysis of experiments, in which, numerous responses have to be optimized at the same time [13]. Based on the criteria kept in software for numerical optimization (Table 5.10.5), only one solution was found and the desirability of 0.984 for the selected model was obtained (Figure 5.10.3). This indicated the reliability of the model for optimization of minimum globule size and PDI for DE NE.

The check point batch was prepared as suggested by the software by selecting constraints for globule size and PDI to be minimized. The predicted and experimental value for the

responses are shown in table 5.10.6. The experimental value for both the responses were found to be in close agreement with the predicted value.

Table 5.10.5. Criteria for selection of desirability of DE NE

Name	Goal	Lower Limit	Upper Limit
X_1	Is in range	5000	15000
X_2	Is in range	2	4
GS	Minimize	71.65	146.1
PDI	minimize	0.109	0.486

Table 5.10.6: Predicted and experimental responses for check point batch of DE NE

Response	Predicted value	Experimental (Mean) value	Percent Prediction Error
Globule size (nm) (Y_1)	72.2821	72.35 ± 0.02	0.0938
PDI (Y_2)	0.118116	0.119 ± 0.01	0.7394

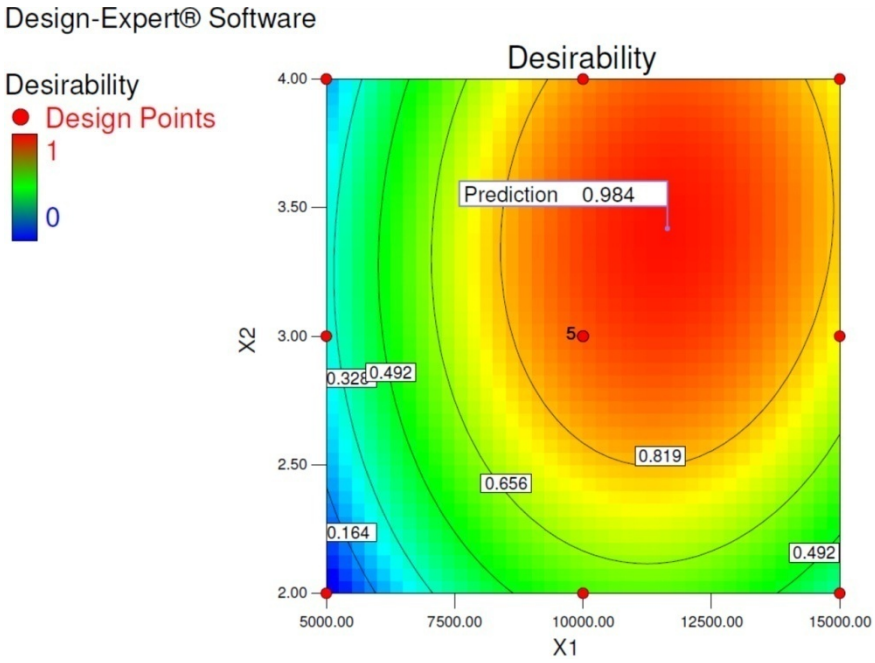

Figure 5.10.3: Desirability plot of optimized batch of DE NE

From the preliminary and optimization studies, the final composition for DE NE comprised of DE (2.0%), Capmul MCM C8 (10.00%), Cremophor EL (10.00%), Transcutol HP (5.00%), and Water (73.00%) was selected for further characterization.

5.10.2. Optimization of NISO NE

The ultrasonication method depends on high-frequency sound waves (above 20 kHz). They can be used to form a nanoemulsion in situ or reduce size of a pre-formed emulsion. Fine

NISO NE was made from its pre-emulsion by ultrasonication method using probe sonicator (Labsonic Sartorius Ltd, India) Bench-top sonicators consist of a piezoelectric probe which generates intense disruptive force at its tip [14] When dipped in a sample, ultrasonic waves produce cavitation bubbles which continue to grow until they implode. This implosion sets up shock waves, which in turn create a jet stream of surrounding liquid, pressurizing dispersed droplets into smaller droplets. Ultrasonicators are amongst the most common lab scale instruments for nanoemulsion production [11].

Probe sonication time (min) and amplitude (%) were taken as variables to check their effect on globule size and PDI as responses for the optimization of NISO NE using 3^2 full factorial design. Globule size and PDI showed the wide variation from 62.35 to 187.65 nm and 0.108 to 0.636 respectively (Table 5.10.7). Total 13 runs were obtained as 4 centre points per block were selected to make the design more robust. When the results were subjected to data analysis by multiple linear regression followed by ANOVA employing Design Expert® software (Version 8.0.3, Suite, Minneapolis, USA), the model fitting was found to be highly significant for both the response variables ($p < 0.0001$). Both responses were found to have good model fitting with insignificant Lack of Fit indicating aptness of the model for future prognostic purposes. The quadratic model was found to be significant for both the responses (Table 5.10.8 and 5.10.9).

Table 5.10.7. Results for 3^2 factorial design of NISO NE

Runs	Probe sonication time (min) (X_1)	Amplitude (%) (X_2)	Globule size (nm) (Y_1)	PDI (Y_2)
1	9	60	71.21 ± 0.65	0.124 ± 0.08
2	9	60	62.35 ± 0.51	0.108 ± 0.05
3	9	40	131.35 ± 0.98	0.542 ± 0.06
4	12	40	156.58 ± 1.03	0.602 ± 0.01
5	9	80	89.54 ± 0.74	0.212 ± 0.07
6	6	80	101.11 ± 0.99	0.411 ± 0.06
7	6	40	187.65 ± 1.12	0.636 ± 0.03
8	9	60	66.14 ± 0.52	0.131 ± 0.01
9	12	80	151.36 ± 1.04	0.342 ± 0.05
10	6	60	132.11 ± 1.01	0.325 ± 0.04
11	12	60	112.32 ± 0.98	0.241 ± 0.02
12	9	60	67.54 ± 0.87	0.145 ± 0.03
13	9	60	74.86 ± 0.76	0.137 ± 0.01

Second order polynomial regression equations were generated to determine the influence of the independent variables on globule size and PDI (Equation 5.10.3. and 5.10.4)

$Y_1=70.50-0.10X_1-22.26X_2+20.33X_1X_2+46.52X_1^2+34.75X_2^2$ .....Eqn 5.10.3

$Y_2=0.13-0.31X_1-0.14X_2-8.750E-003X_1X_2+0.14X_1^2+0.23X_2^2$ .....Eqn 5.10.4

The regression coefficients having $p<0.05$ are highly significant. The terms having coefficients with $p>0.05$ are least contributing in the prediction of response. In case of GS, X_2, X_1X_2, X_1^2, X_2^2 are significant model terms and X_1, X_2, X_1^2, X_2^2 are significant model terms in case of PDI.

Table 5.10.8: Results of ANOVA for GS of NISO NE

Source	Sum of Squares	df	Mean square	F Value	p-value prob>F	
Model	19500.76	5	3900.15	50.39	<0.0001	Significant
X_1	0.062	1	0.062	8.012E-004	0.9782	
X_2	2973.49	1	2973.49	38.41	0.0004	
X_1X_2	1653.24	1	1653.24	21.36	0.0024	
X_1^2	5977.64	1	5977.64	77.22	<0.0001	
X_2^2	3335.60	1	3335.60	43.09	0.0003	
Residual	541.85	7	77.41	--	--	
Lack of Fit	449.77	3	149.92	6.51	0.0501	Not Significant

Table 5.10.9: Results of ANOVA for PDI of NISO NE

Source	Sum of Squares	df	Mean square	F Value	p-value prob>F	
Model	0.43	5	0.086	135.36	<0.0001	Significant
X_1	5.828E-003	1	5.828E-003	9.15	0.0192	
X_2	0.11	1	0.11	173.88	<0.0001	
X_1X_2	3.063E-004	1	3.063E-004	0.48	0.5103	
X_1^2	0.052	1	0.053	82.55	<0.0001	
X_2^2	0.15	1	0.15	233.39	<0.0001	
Residual	4.457E-003	7	6.367E-004	--	--	
Lack of Fit	3.657E-004	3	1.222E-003	6.19	0.0553	Not Significant

The predicted R-Squared for both the responses were in reasonable agreement with the adjusted R-Squared indicating that the selection and model fitting were acceptable (Table 5.10.10).

Table 5.10.10: Model Statistics for Y1 and Y2 responses for NISO NE using 3^2 full factorial design

Response	Model	Model F-value	R-Squared	Adjusted R-Squared	Predicted R-Squared	Lack of Fit p-value	Std. Dev.
Y1	Quadratic	50.39	0.9730	0.9537	0.7911	0.0510	8.80
Y2	Quadratic	136.80	0.9898	0.9825	0.9175	0.0553	0.025

Influence of Probe sonication time on GS and PDI

The probe sonication time had significant effect on globule size and was the crucial step in globule size reduction. Equation 5.10.3 and results from table 5.10.7 revealed that globule size was negatively impacted by the probe sonication time. The globule size steadily decreased on increasing the sonication time. This might be attributed to two factors- firstly the energy provided and secondly the shear force exerted during sonication. Both these factors lead to deformation and fragmentation of coarse dispersion into nano-droplets. It is expected to have small droplets size with increasing sonication time [15]. The globule size decreased gradually as sonication time increased from 6 to 9 min. However, further increase of sonication time from 9 to 12 min increased the globule size. This might be due to the high kinetic energy of small droplets which led to aggregations of globules and increase globule size. Hence, 9 min were concluded to be the probe sonication time for achieving minimum globule size.

Equation 5.10.4 and results from table 5.10.7 revealed that PDI was negatively influenced by probe sonication time. The negative coefficients of variables X_1 and X_2 indicated an opposite effect on PDI. As sonication time increased from 6 to 9 min PDI value decreased, however, further increase in sonication time from 9 to 12 led to increase in PDI. Higher PDI in the formulation indicates non-uniform globule size distribution. Uniform distribution was observed when value for PDI was observed to be at lower side.

Influence of Amplitude on GS and PDI

Sonication amplitude has a negative impact on the globule size, i.e. with increase in the sonication amplitude there is decrease in the globule size as shown in the equation 5.10.3. An increase in the sonication amplitude leads to reduction in globule size due to the disruption of the globules with increase in energy density. Increase in power amplitude induces stronger mechanical vibration and generates more cavities. A large number of such cavities lead to more powerful shockwaves thereby resulting in smaller emulsion droplets [16]. As the amplitude increased from 40 to 60%, (Table 5.10.7) the globule size decreased due to increase in shear which caused breakdown of bigger particles.

Similarly, PDI was found to be decreased on increasing amplitude up to 60%. The globule size and PDI of nanoemulsion showed minimum size and lowest PDI at an intermediate amplitude which then increased at higher power levels i.e. 80%. This effect is described as "over-processing" which is caused by increase in emulsion globule coalescence at higher shear rates [1]. Hence, 60% of amplitude was considered as optimum condition to obtain nanoemulsion with desired globule size and uniform distribution.

Contour plots and response surface analysis

The relationship between independent and dependent variables were explicated using contour and response surface plots. Contour and response surface plots were generated between the two variables: Probe sonication time (X_1) and amplitude (X_2) for GS and PDI as responses. In both the cases, the contour plot formed oval shape (Figure 5.10.4). From response surface plots (Figure 5.10.5), it was observed that as X_1 increased up to 9.0, globule size and PDI decreased but increased on further increase in X_1. Similar effects were observed with X_2.. Hence, the mid value of both variables showed the desired responses .

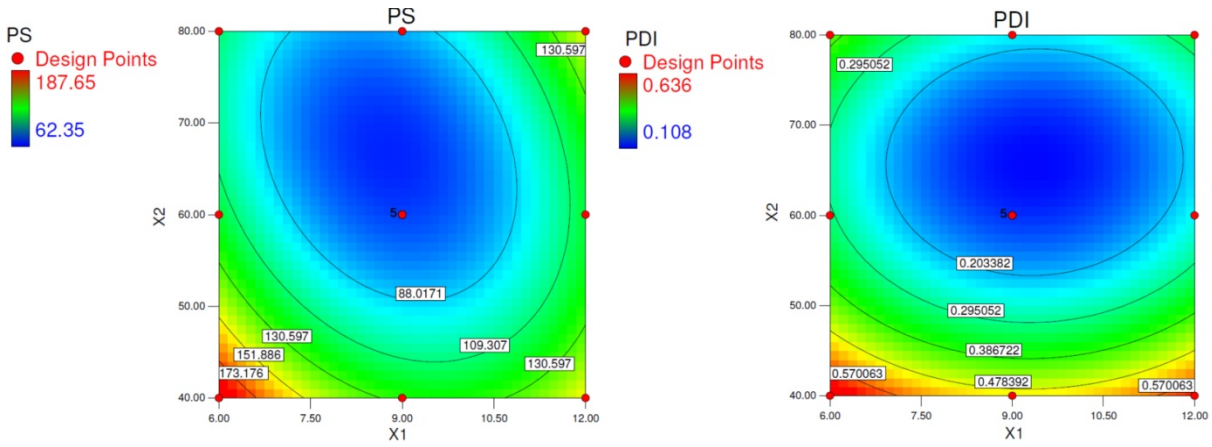

Figure 5.10.4. Contour plots showing effect of independent variables on GS and PDI for NISO NE

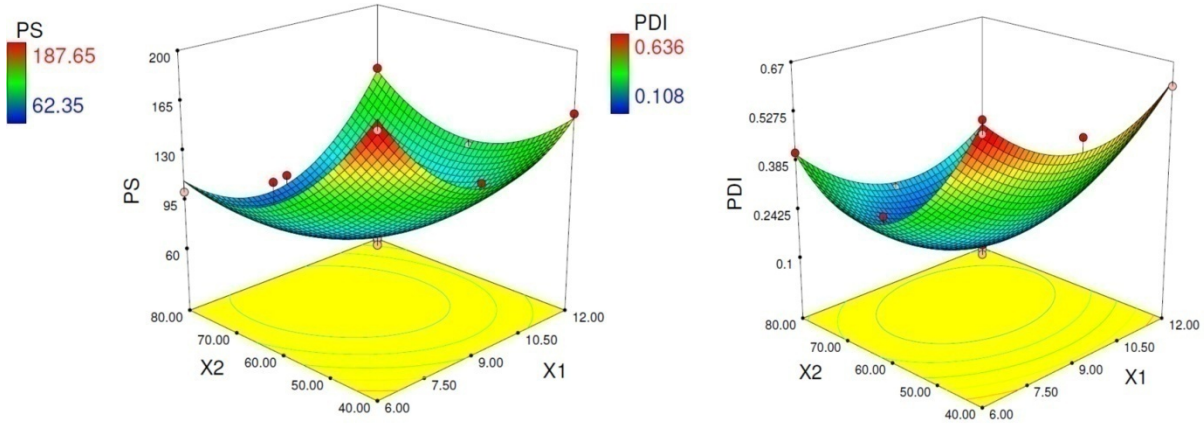

Figure 5.10.5. Response surface plots showing effect of independent variables on GS and PDI for NISO NE

Check point analysis/desirability function

A check point analysis was performed to confirm the utility of the established contour plots and reduced polynomial equation in the preparation of NE. The check point batch was prepared as suggested by software by selecting constraints for GS and PDI to be minimum. The predicted and experimental value for the responses are shown in table 5.10.11. The experimental values for both the responses were found to be in close agreement with the predicted value.

Table 5.10.11: Predicted and experimental responses for check point analysis of NISO NE

Response	Predicted value	Experimental (Mean) value	Percent Prediction Error
Globule size (nm) (Y_1)	67.0127	67.12± 0.03	0.1598
PDI (Y_2)	0.113381	0.116± 0.01	0.022

Desirability criteria obtained using Design Expert software (version 8.0.3) was used to find out optimized formulation parameters. Desirability function can be used to validate selected model. The optimum formulation offered by the software based on desirability was found at targeted level of X_1 and X_2 respectively. Desired criteria included minimum GS and minimum PDI (Table 5.10.5). From the software, desirability of 0.976 for the selected model was obtained (Figure 5.10.6) which was near to 1 and indicated suitability of the designed factorial model.

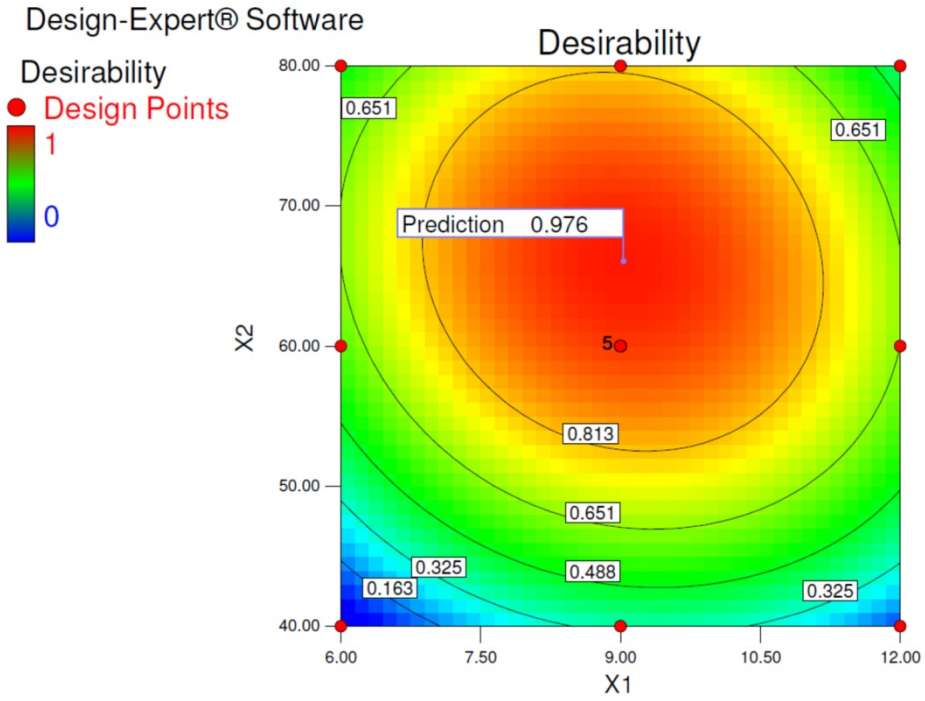

Figure 5.10.6. Desirability plot for optimized batch of NISO NE

From the preliminary and optimization studies, the final composition for NISO NE comprised of NISO (1.00%), Peceol (10.00%), Cremophor EL (10.00%), Transcutol HP (10.00%) and Water (69.00%) was selected for further characterization.

5.11. Characterization of optimized DE and NISO NE

5.11.1. Globule size, poly dispersity index (PDI)

Globule size is considered to be an important parameter in formulation of nanoemulsions because dissolution rate and absorption of a compound is determined by the globule size of the formulation [12]. The optimized DE NE and NISO NE had globule size of 71.65 ± 1.02 nm (Figure 5.11.1) and 62.35 ± 2.55 nm (Figure 5.11.2) respectively. PDI plays an important role in the formulation of nanoemulsions as it determines the homogeneity of the nanoemulsion globules. PDI close to 0 is always desirable. Higher PDI in the formulation indicates non-uniform globule size distribution. PDI for both the DE NE and NISO NE was 0.109 ± 0.02 (Figure 5.11.1) and 0.108 ± 0.01 (Figure 5.11.2) respectively. This revealed that both the formulations exhibited uniform globule size distribution.

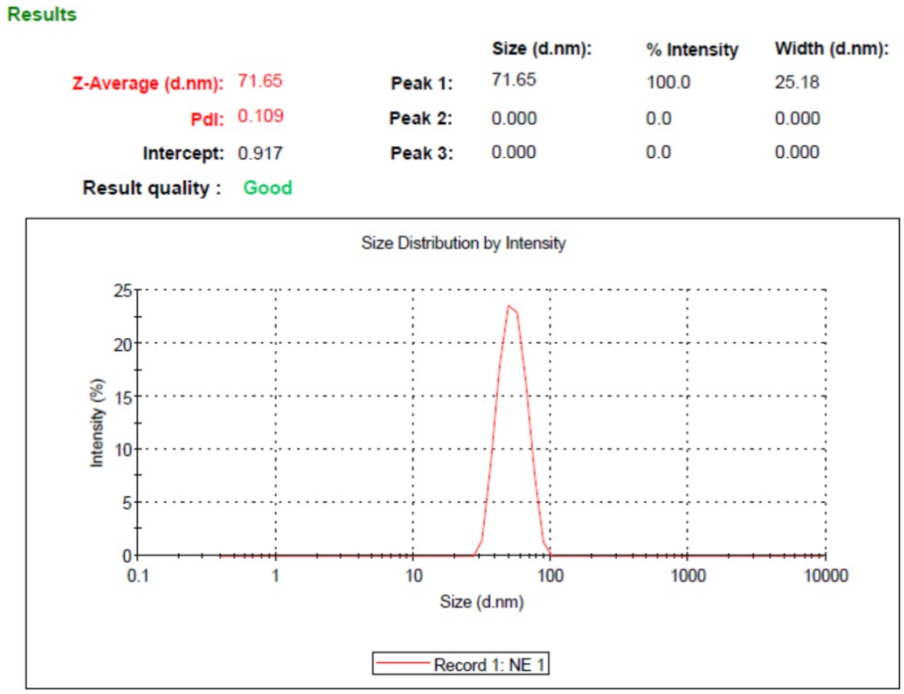

Figure 5.11.1. Globule size for optimized batch of DE NE

Results

		Size (d.nm):	% Intensity	Width (d.nm):
Z-Average (d.nm): 62.35	Peak 1:	62.35	100.0	20.73
PdI: 0.108	Peak 2:	0.000	0.0	0.000
Intercept: 0.906	Peak 3:	0.000	0.0	0.000

Result quality : Good

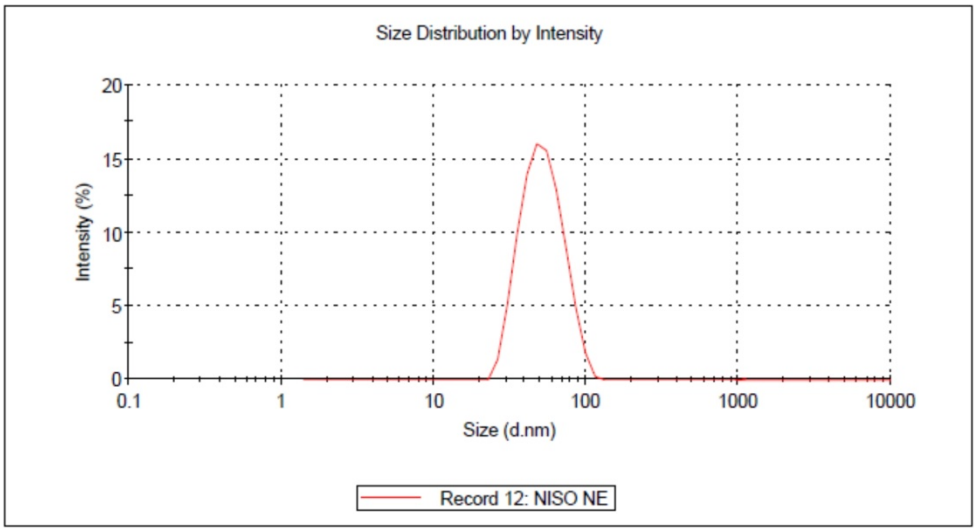

Figure 5.11.2. Globule size for optimized batch of NISO NE

5.11.2. Measurement of Zeta potential

The zeta potential is indicative of the charge on the surface of the particles and a higher zeta potential value ensures that there is no phase separation, while a value closer to zero leads to risk of coalescence, thus suggesting instability [17]. Zeta potential should usually reach an absolute value ±30 mV to obtain stable emulsion by preventing flocculation and coalescence of nanosized droplets [18]. Zeta potential of DE NE and NISO NE were found to be -19.6 ± 2.1mV and -26.2 ± 3.6mV respectively (Figure 5.11.3 and 5.11.4). The high negative values of the zeta potential indicate strong electrostatic repulsion between the globules will prevent their aggregation and thereby stabilize the nanoemulsions.

Results

		Mean (mV)	Area (%)	Width (mV)
Zeta Potential (mV): -19.6	**Peak 1:**	-19.6	100	8.66
Zeta Deviation (mV): 8.66	**Peak 2:**	0.00	0.0	0.00
Conductivity (mS/cm): 0.0521	**Peak 3:**	0.00	0.0	0.00

Result quality : Good

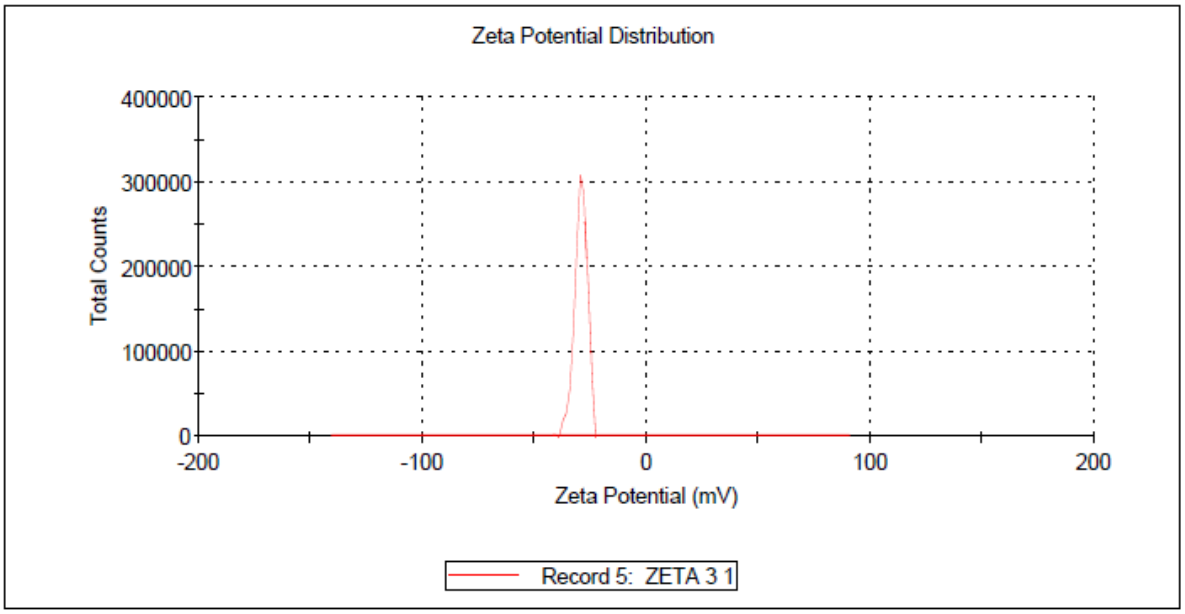

Figure 5.11.3. Zeta potential of optimized batch of DE NE

Results

		Mean (mV)	Area (%)	Width (mV)
Zeta Potential (mV): -26.2	**Peak 1:**	-26.2	100.0	8.12
Zeta Deviation (mV): 8.12	**Peak 2:**	0.00	0.0	0.00
Conductivity (mS/cm): 0.0452	**Peak 3:**	0.00	0.0	0.00

Result quality : Good

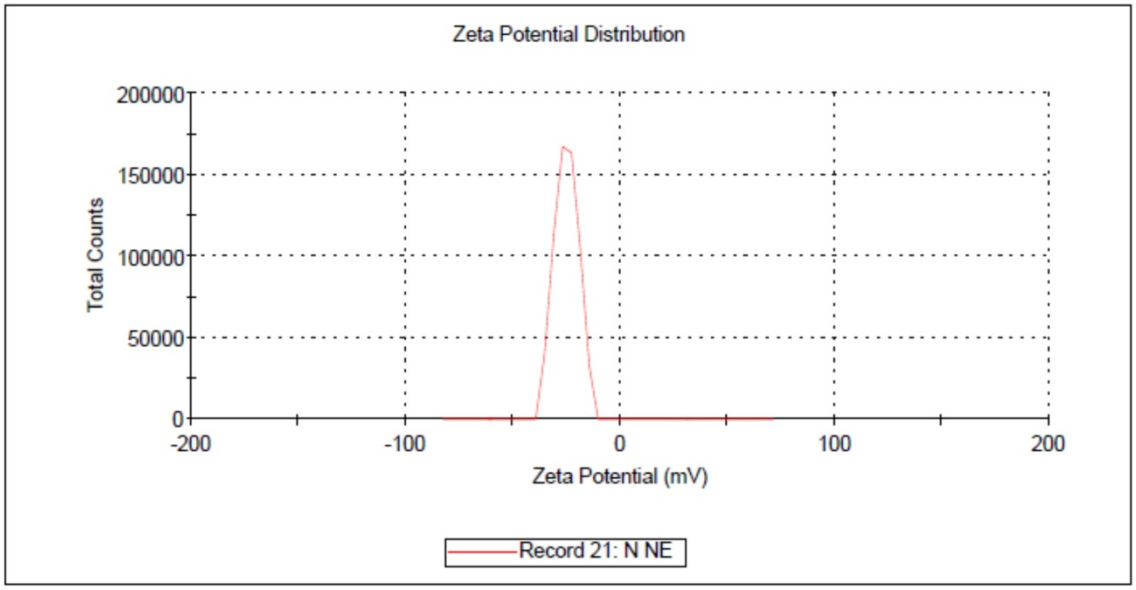

Figure 5.11.4. Zeta potential of optimized batch of NISO NE

5.11.3. Drug content

The drug content of DE NE and NISO NE were found to be 98.04± 2.57% and 98.87± 2.12% respectively suggesting uniform distribution of drug in the internal phase of both the nanoemulsions.

5.11.4. pH

The pH of DE NE and NISO NE was found to be 6.2± 0.3 and 6.6± 0.2 respectively demonstrating aptness for oral administration.

5.11.5. Morphological examination using Transmission Electron Microscopy (TEM)

TEM analysis is important in order to study the morphology of the oil droplets in the nanoemulsion formulations and to visualize any precipitation of the drug upon addition of the aqueous phase. As observed in the TEM images, the globules were discrete and spherical with no signs of coalescence and had diameter ranging from 45 to 75 nm and 60 to 90 nm for DE NE and NISO NE respectively (Figure 5.11.5 and 5.11.6). No sign of drug precipitation was observed inferring the stability of nanoemulsions even after dilution. The globule size observed in the TEM images were in accordance with result obtained by Zetasizer for both the formulations.

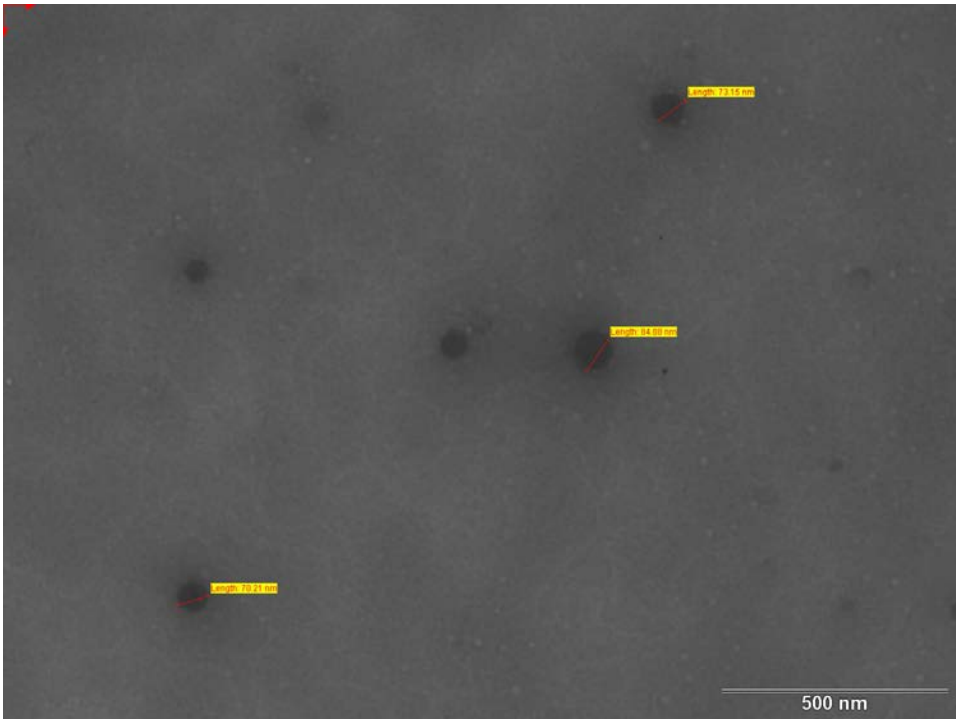

Figure 5.11.5. Transmission Electron Microscopy (TEM) image of optimized batch for DE NE

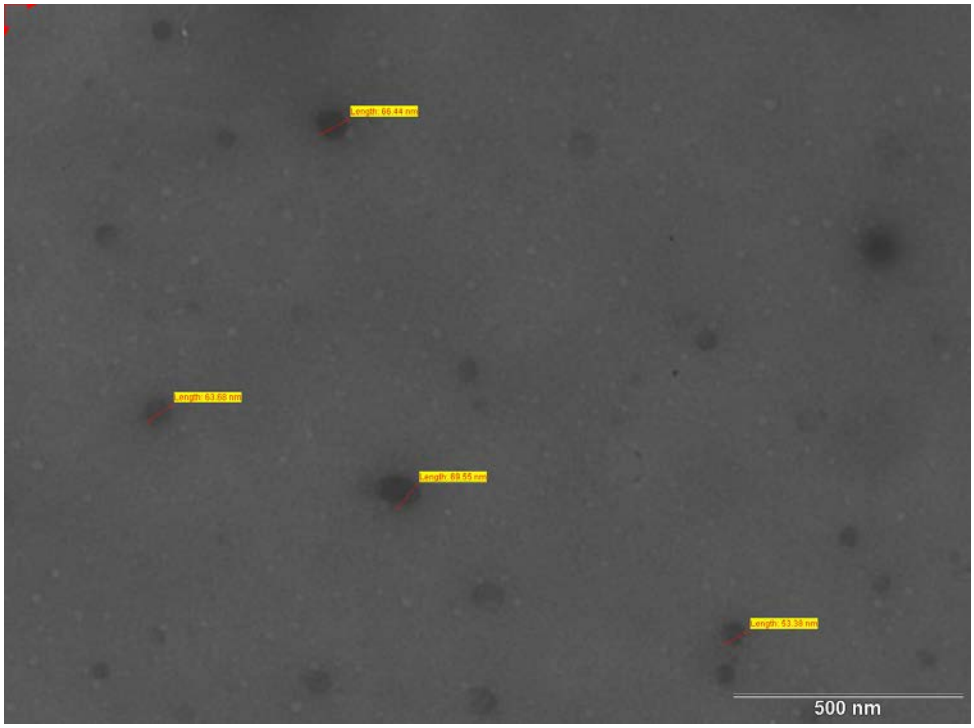

Figure 5.11.6. Transmission Electron Microscopy (TEM) image of optimized batch for NISO NE

5.11.6. Conductivity

The conductivity of DE NE and NISO NE was 156.36 and 161.54 µS/cm respectively. Oil-in-water (O/W) NE are highly conductive since water is in the external phase. This high conductivity values confirmed the O/W structure of the prepared nanoemulsions [19].

5.11.7. Viscosity

The viscosity of nanoemulsions is a function of the surfactant, water and oil components and their concentrations. It also depends on the type of nanoemulsion. Increasing the water content lowers the viscosity of in both o/w and w/o type of nanoemulsions, while decreasing the amount of surfactant and co surfactant increases viscosity of w/o type of nanoemulsions whereas decreases viscosity of o/w type of emulsion. Viscosity is important parameter for stability as well as efficient release of drug from nanoemulsions [20]. The viscosity of the NISO-NE and DE-NE were found to be 23.69± 1.84 cps and 12.02± 1.01 cps respectively. The viscosity of nanoemulsion formulations were found very low which is the expected characteristic of any nanoemulsion [21].

5.11.8. Thermodynamic stability assessment

Thermodynamic stability confers long shelf life to the nanoemulsion when subjected to heating cooling cycle (to check the stability at higher temperature), freeze thaw cycle (to

check stability at low temperature) and centrifugation studies (to check stability at high shear) [12]. Both the optimized formulations of the NISO-NE and DE-NE were found to be stable as no phase separation, turbidity, creaming or cracking was observed upon temperature variations and the formulations could withstand high speed centrifugation at 5000 rpm for 20 minutes.

5.11.9 Fourier transform infrared (FTIR) spectroscopy

The FTIR spectra of optimized formulation of DE NE and NISO NE, pure drugs and placebo mix were recorded. Individual IR spectra of DE (Figure 4.6.3), placebo mix for DE NE (Figure 5.11.7) and DE NE (Figure 5.11.8) were recorded. Similarly, IR spectra of NISO (Figure 4.6.4), placebo mix for NISO NE (Figure 5.11.9) and NISO NE (Figure 5.11.10) were recorded. Since the formulation contains water , prominent -OH peak was observed at 3346cm^{-1} for both DE and NISO. Both the drugs contain secondary amine and ester functional groups. So these contain -NH stretching vibrations in the region of 3500-3100 cm^{-1} and free -OH peak appears in the region of 3400-3200 cm^{-1}. This leads to overlapping of some peaks. Further, it was observed that the principal peaks of DE and NISO as shown in Table 5.11.1 and 5.11.2 respectively, were retained as such in the spectra of DE NE (Figure 5.11.8) and NISO NE (Figure 5.11.10), thereby indicating the absence of any significant interaction or incompatibility between the drug and excipients used in the formulations of NE.

Table 5.11.1: Functional groups along with their wave numbers for DE NE

Functional Groups	Wave number (cm^{-1})	
	Observed	**Reference**
Free -OH	3346	3400-3200
-NH_2 (Primary amine)		
-NH (Stretching)	3456	3500-3100
-NH (Bending)	1547	1640-1550
-OCO- (Ester)		
C=O (stretching)	1740	1750-1730
-NH (Stretching)	3456	3500-3100
-CO (Bending)	1147	1300-1000
-NH- (Secondary Amine)		
-NH (Stretching)	3456	3500-3100
-CN (Bending)	1249	1350-1000
-NHCO- (Amide)		
C=O (stretching)	1681	1680-1630
-NH (Stretching)	3456	3500-3100
Aromatic ring		
Stretching	3263	3150-3050
Bending	1611	1600-1475
Alkanes (-CH_3)		
-CH (Stretching)	2980	3000-2850
-CH (Bending)	1336	1450-1375

Table 5.11.2 Functional groups along with their wave numbers for NISO NE

Functional Groups	Wave number (cm^{-1})	
	Observed	**Reference**
Free -OH	**3346**	**3400-3200**
-NH- (Secondary Amine)		
-NH (Stretching)	3327	3500-3100
-NH (Bending)	1641	1640-1550
-CN (Bending)	1346	1350-1000
-OCO- (Ester)		
C=O (stretching)	1711	1750-1730
-NH (Stretching)	3146	3500-3100
-CO (Bending)	1310	1310-1000
Aromatic ring		
Stretching	3257	3150-3050
Bending	1611	1600-1475
Alkanes ($-CH_3$)		
-CH (Stretching)	2980	3000-2850
-CH (Bending)	1463	1450-1375

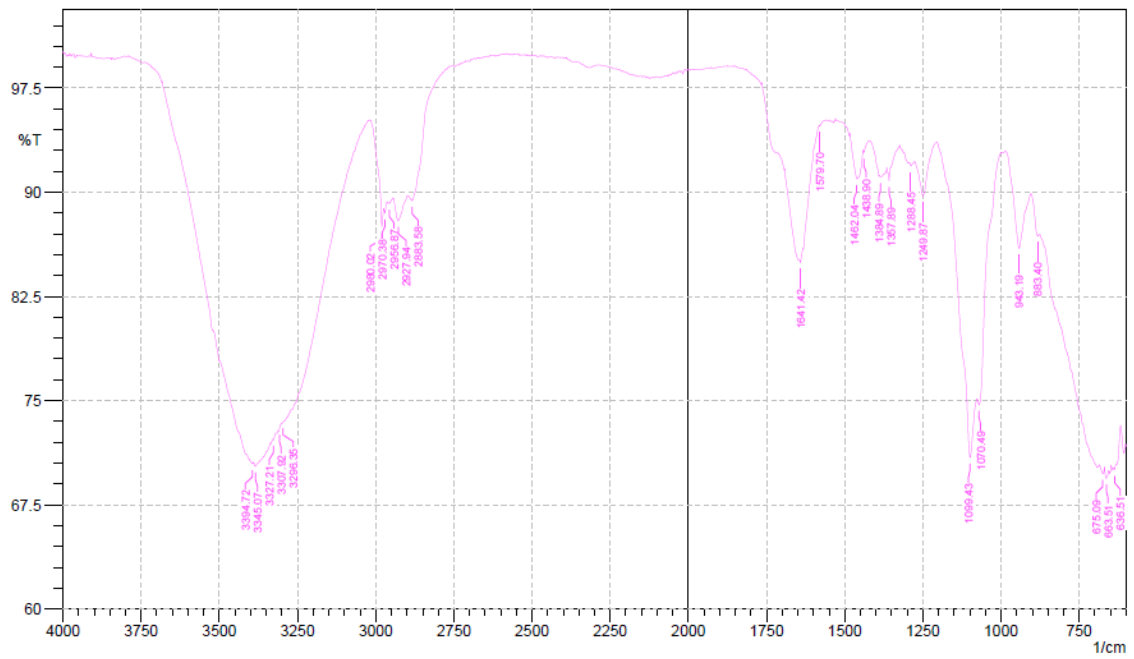

Figure 5.11.7: FTIR spectrum of placebo mix for DE NE

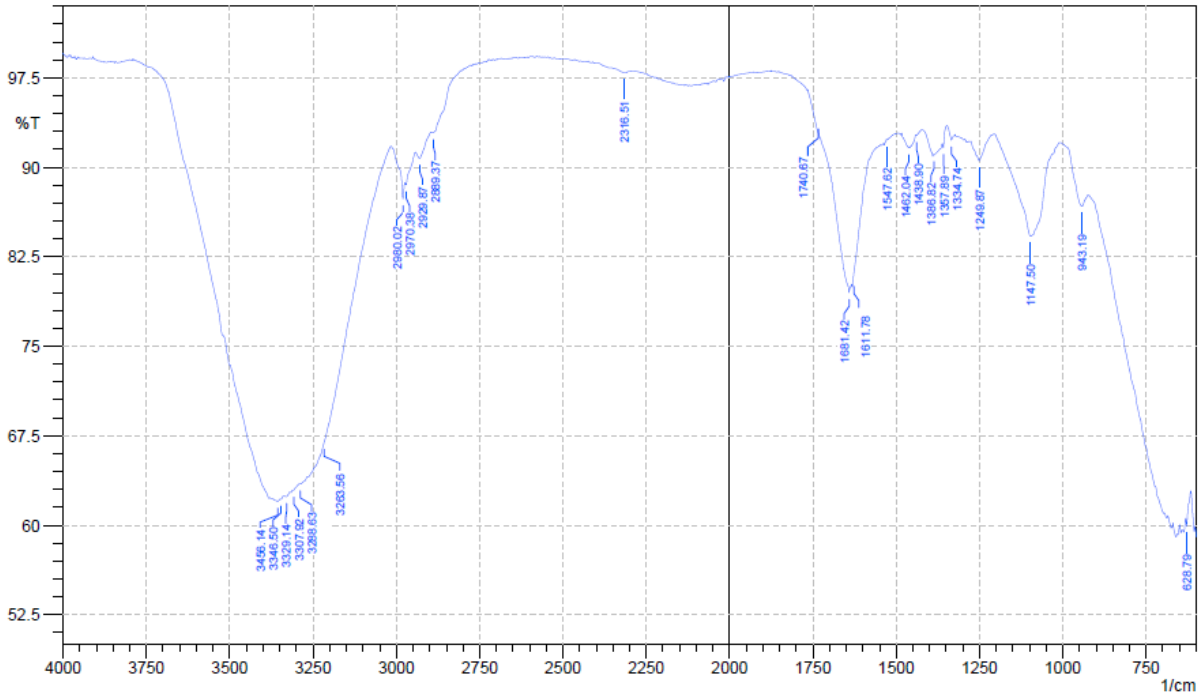

Figure 5.11.8: FTIR spectrum of DE NE

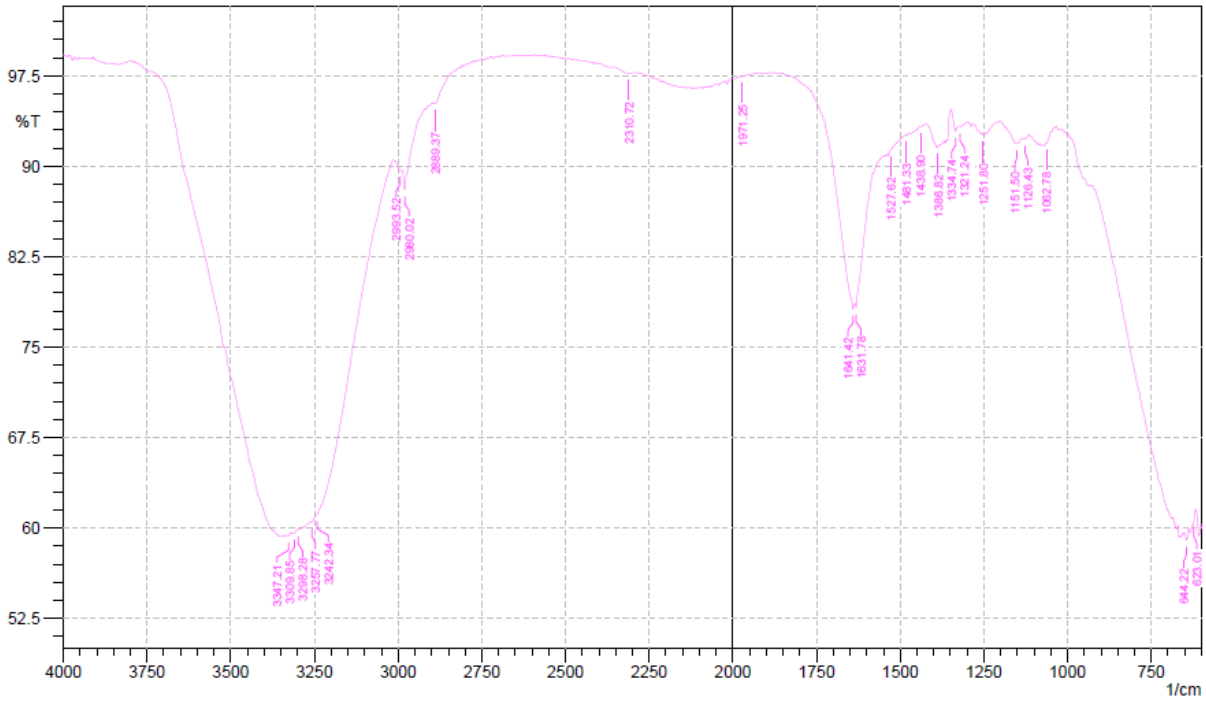

Figure 5.11.9: FTIR spectrum of placebo mix for NISO NE

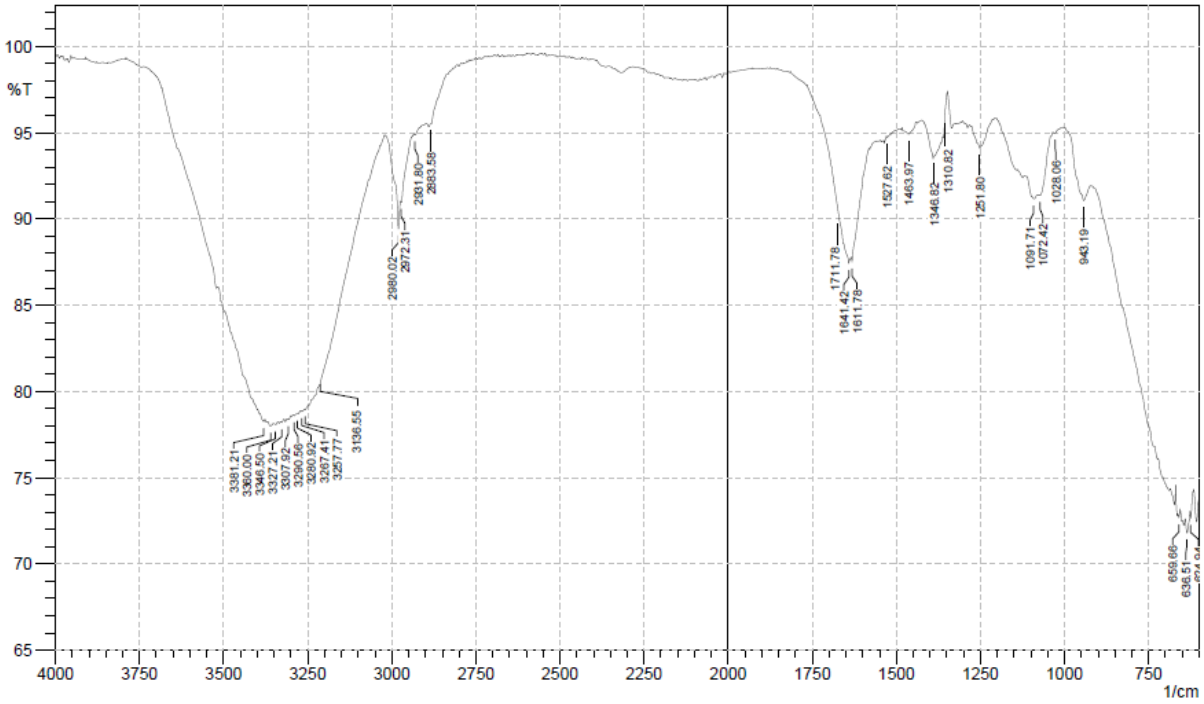

Figure 5.11.10: FTIR spectrum of NISO NE

5.11.10. Drug release studies

5.11.10.1. *In vitro* dissolution study

5.11.10.1.1. *In vitro* dissolution study of DE NE

The *in vitro* release profiles of DE NE and plain drug suspension in 0.01N HCl and pH 6.8 phosphate buffer are shown in Figure 5.11.11. The *in vitro* release studies showed increase in drug release as compared to plain drug suspension in both the media.

Plain drug suspension showed only 35.05±0.44% drug release while DE NE formulation showed almost complete release of 98.33±0.92% in 60 min in 0.01N HCl. This high and fast drug release could be attributed to enhanced solubility and dissolution rate of DE which in turn can be due to low droplet size and surface properties of the nanoemulsion.

In case of pH 6.8 phosphate buffer, cumulative drug release was only 9.23± 3.02% from drug suspension and 67.53± 3.11% from DE-NE in 60 min (Figure 5.11.11). In each release media, the release of DE from NE was higher than that from free drug suspension, which could be attributed to the solubilising effect of nanoemulsion while plain drug suspension was characterized by slow and poor dissolution. The release of DE from NE in 0.01N HCl was much higher than that at pH 6.8 phosphate buffer, which could result from the higher solubility of DE at low pH values.

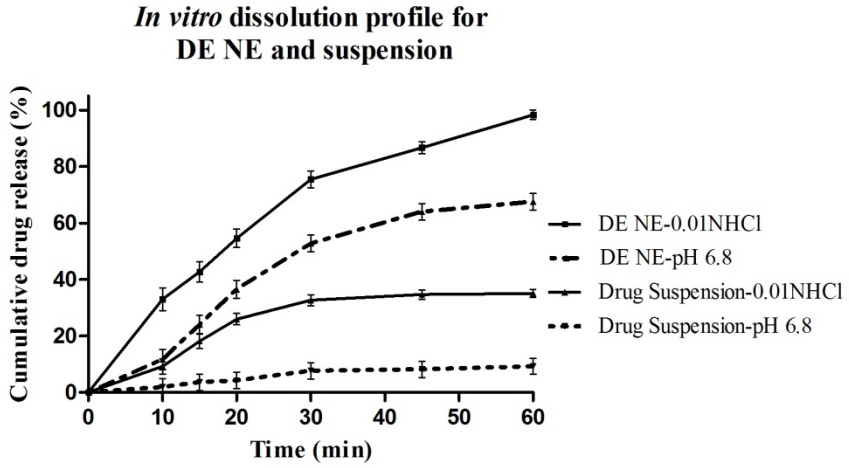

Figure 5.11.11. *In vitro* dissolution profile of DE NE and drug suspension in 0.01N HCl and pH 6.8 phosphate buffer

5.11.10.1.2. *In vitro* dissolution study of NISO NE

The dissolution of NISO NE and pure drug suspension were performed in 0.1N HCl with 0.5% SLS and pH 6.8 phosphate buffer with 0.5% SLS as shown figure 5.11.12. In case of NISO NE, the drug release after 60 min was 99.20± 2.04% in 0.1N HCl+ 0.5% SLS and 15.10± 2.63% from pure drug suspension while 98.31± 3.17% of release was observed from NISO NE in pH 6.8 Phosphate buffer with 0.5% SLS and 13.92± 2.88% from drug suspension. Faster release was observed in both the media for NE as compared to drug suspension. This might be because of small globule size, and eventually higher surface area of nanoemulsions, which permit faster rate of drug release than plain drug suspension.

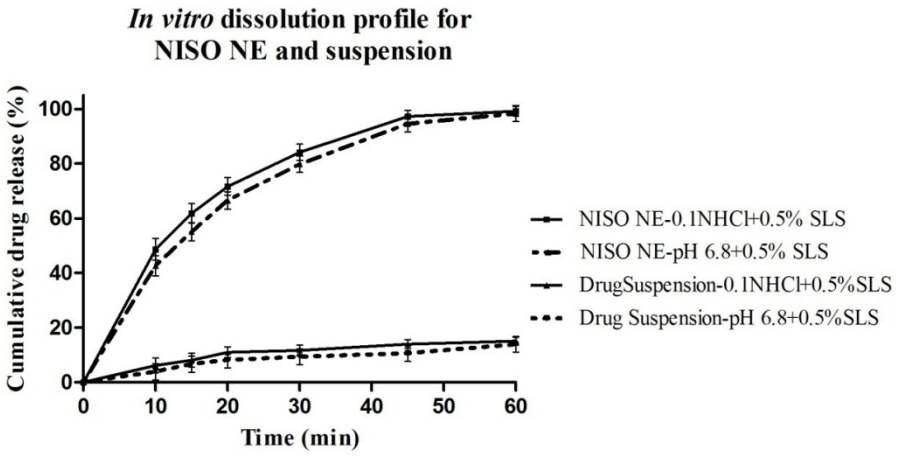

Figure 5.11.12. *In vitro* dissolution profile of NISO NE and drug suspension in 0.01N HCl and pH 6.8 phosphate buffer

5.11.10.2. *In vitro* diffusion study

5.11.10.2.1. *In vitro* diffusion study of DE NE

The cumulative percentage diffusion was higher for the DE NE than for the plain drug suspension. As seen from figure 5.11.13, higher amount of the drug was diffused at 300 min. from the DE NE (98.97± 2.56% and 70.02± 3.12%) as compared to the plain drug suspension (37.14± 1.96 % and 15.87± 2.18%) in 0.01N HCl and in pH 6.8 phosphate buffer respectively. The high surface area due to smaller globule size and the fact that the drug is in a solubilised state in NE are thought to be the attributing factors for its higher diffusion compared to plain drug suspension. However, DE being a weakly basic drug with pH-dependent solubility, justify the results obtained.

The release profiles were then fitted into various mathematical models to determine the best-fit model (Table 5.11.3). The r^2 value were found to be highest for Higuchi model (r^2 = 0.999) in both 0.01N HCl while in pH 6.8 phosphate buffer (Figure 5.11.14 and 5.11.15). The drug release is from oil globules and its geometry was considered to be sphere and the type of drug release mechanism was defined. The value for release component 'n' was between 0.43 and 0.85, indicating Non- Fickian diffusion release kinetics [22].

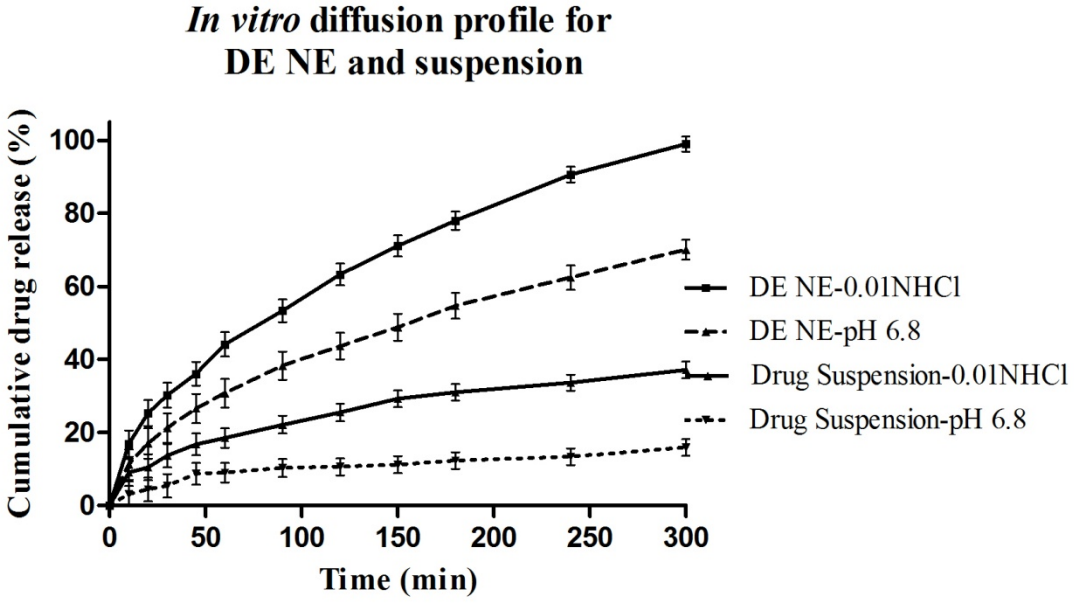

Figure 5.11.13. *In vitro* diffusion profile of DE NE and drug suspension in 0.01N HCl and pH 6.8 phosphate buffer

Table 5.11.3. Regression coefficient of various *in vitro* release models for DE NE

Release models	0.01N HCl	pH 6.8 Phosphate Buffer	n' values for sphere geometry	Drug release mechanism
	R^2			
Zero order	0.927	0.927	0.43	Fickian diffusion
First order	0.886	0.987		
Hixson-Crowell	0.981	0.973	0.43 < n < 0.85	Non-fickian (anomalous) diffusion
Higuchi	0.999	0.999		
Korsmeyer-Peppas (Release component -'n')	0.998 (0.521)	0.998 (0.532)	0.85	Case-II transport

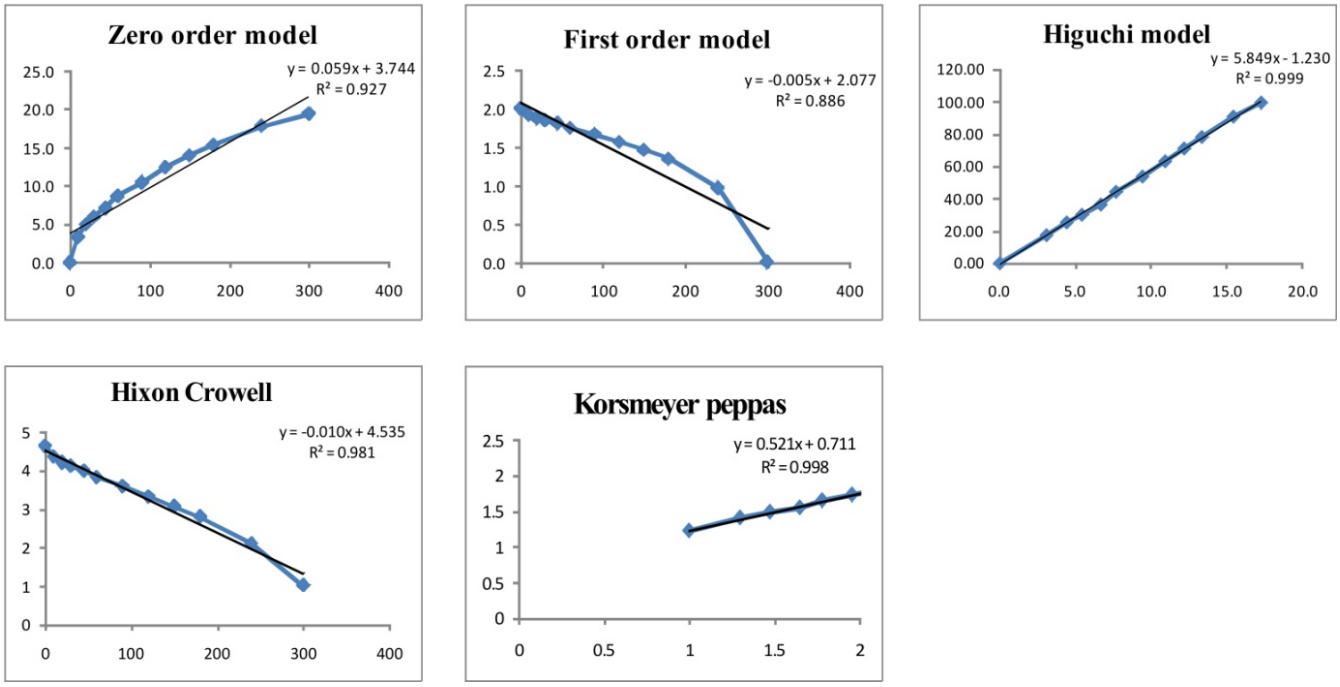

Figure 5.11.14. Release kinetics curves in 0.01N HCl for DE NE

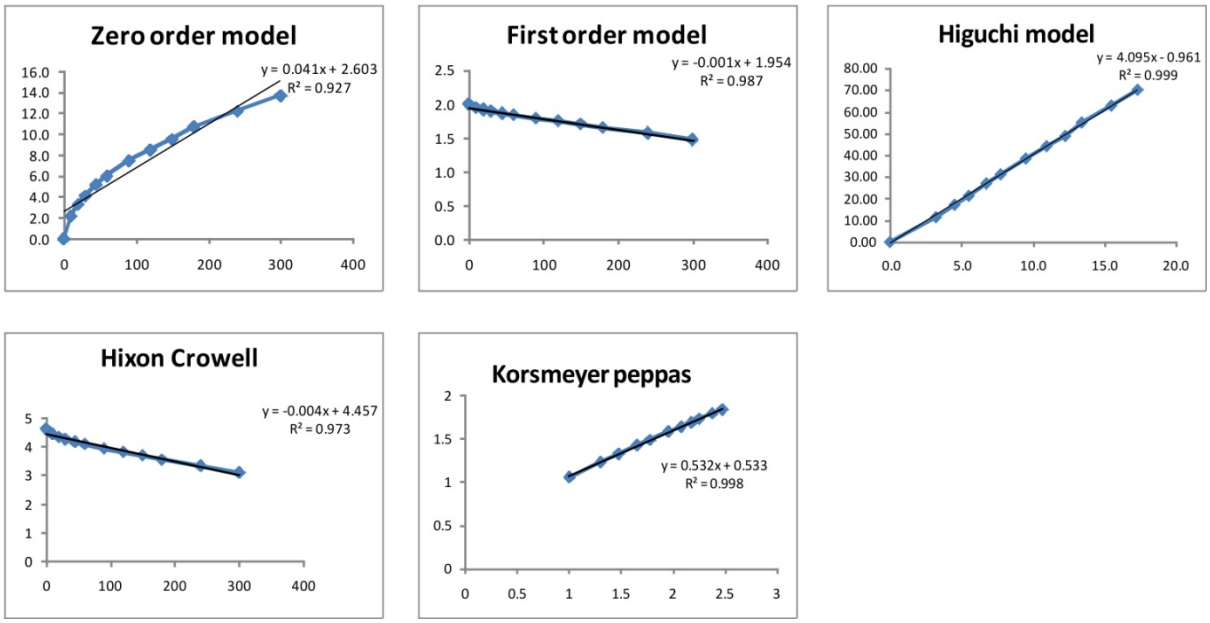

Figure 5.11.15. Release kinetics curves in pH 6.8 phosphate buffer for DE NE

5.11.10.2.2. *In vitro* diffusion study of NISO NE

The *in vitro* diffusion profiles of NISO NE and plain drug suspension are as given in Figure 5.11.16. The *in vitro* diffusion study showed significant increase in drug release from NE formulations as compared to plain drug suspension. In case of 0.1N HCl + 0.5% SLS, the cumulative percent drug released after 300 min was 98.51± 2.64% and 29.73± 2.15% from NISO NE and drug suspension respectively. Similarly, for pH 6.8 Phosphate buffer + 0.5% SLS, 99.04 ± 3.11% and 31.76± 2.62% drug released from NISO NE and drug suspension respectively. This could be attributed to enhanced solubility and dissolution rate of NISO from NE which in turn can be due to low globule size and high surface properties of the prepared NE.

The release profiles were then fitted into different exponential equations such as Zero order, First order, Higuchi, Hixon Crowell and Korsmeyer- Peppas to characterize the release. It was found that drug release from NISO NE in both media followed Higuchi model (r^2=0.996 and r^2=0.993 respectively) as shown in figure 5.11.17 and 5.11.18 respectively. Value of '*n*' indicates that both plain drug suspension and NISO NE followed fickian diffusion as the release component values were between 0.43<n<0.85 (Table 5.11.4).

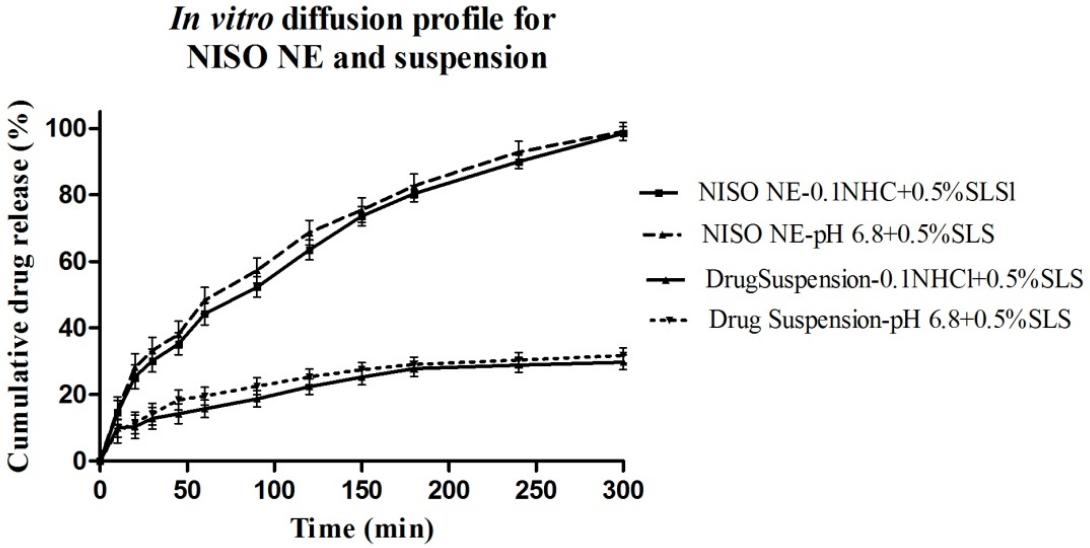

Figure 5.11.16. *In vitro* diffusion profile of NISO NE and drug suspension in 0.01N HCl and pH 6.8 phosphate buffer

Table 5.11.4. Regression coefficient of various *in vitro* release models for NISO NE

Release models	0.1N HCl+0.5% SLS	pH 6.8 Phosphate Buffer + 0.5% SLS	n' values for sphere geometry	Drug release mechanism
	R^2			
Zero order	0.921	0.896	0.43	Fickian diffusion
First order	0.921	0.921		
Hixson-Crowell	0.989	0.991	0.43<n<0.85	Non-fickian (anomalous) diffusion
Higuchi	0.996	0.993		
Korsmeyer-Peppas (Release component -'n')	0.993 (0.550)	0.985 (0.534)	0.85	Case-II transport

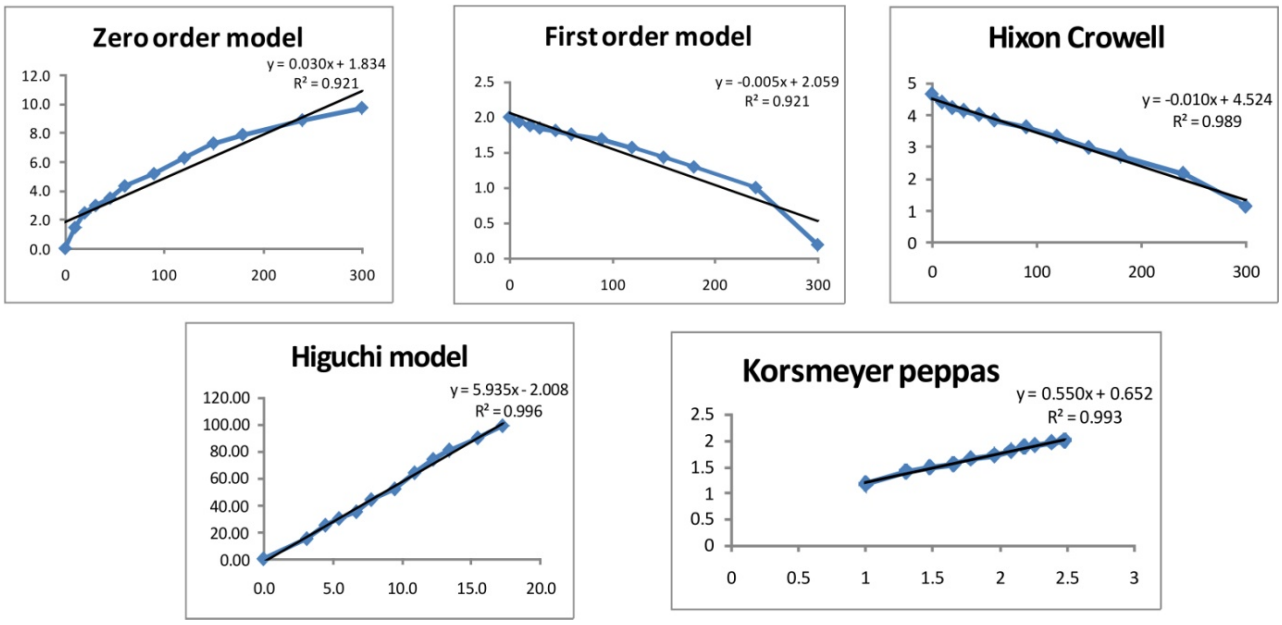

Figure 5.11.17. Release kinetics curves in 0. 1N HCl for NISO NE

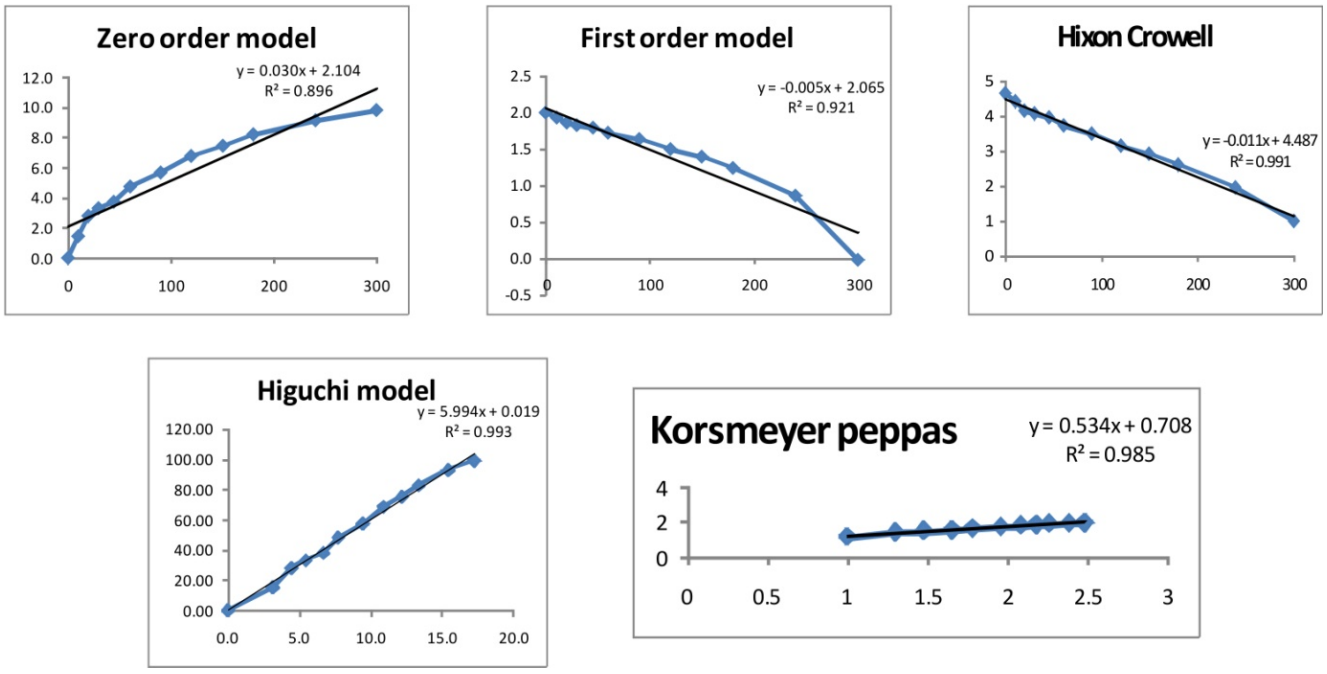

Figure 5.11.18. Release kinetics curves in pH 6.8 phosphate buffer for NISO NE

5.11.10.3. *Ex vivo* release study

5.11.10.3.1. *Ex vivo* release study of DE NE

The cumulative % drug release from rat stomach and intestine are shown in Figure 5.11.19. It was observed that 97.25± 3.61% drug diffused from the NE formulation through stomach in 300 min while from plain drug suspension, the diffusion was found to be only 28.86± 3.21%. Thus, the amount of the drug diffused through the biological membrane increased when it

was given in the form of a NE. This might be due to the hydration of the inner tissue layer due to external water phase of the NE resulting in high diffusivity of lipophilic drug as droplet size approaches to molecular dispersion [19]. Intestinal diffusion was relatively slower than stomach i.e. 68.64 ± 3.36% drug was diffused from the DE NE and 11.75± 2.11 % from plain drug suspension which could be attributed to the higher solubility of DE (weak base) in acidic conditions. Altogether such a pattern is desirable for our purpose as significant amount of drug will be carried to the intestinal portion inside the nanoemulsion globules.

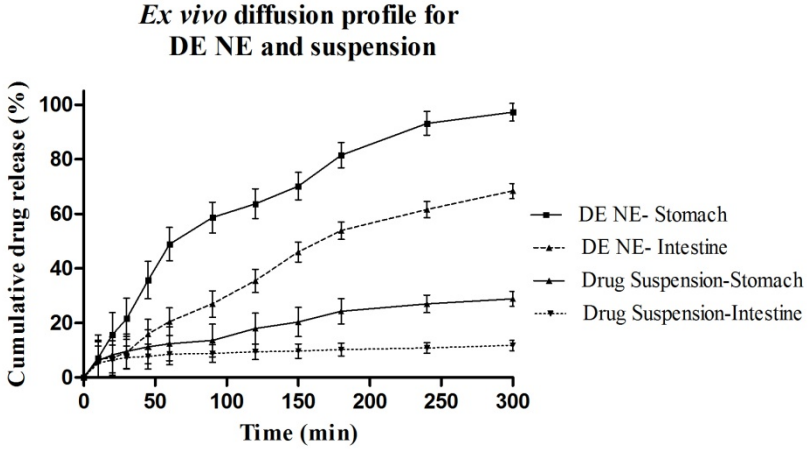

Figure 5.11.19. *Ex vivo* release study of DE NE and drug suspension from rat stomach and intestine tissue.

5.11.10.3.2. *Ex vivo* diffusion study of NISO NE

Ex vivo release study mimics the *in vivo* conditions and predicts transport of the formulation across the gastro intestinal membrane. The cumulative % drug release from rat stomach and intestine are as shown in Figure 5.11.20. The total drug diffusion from both the stomach (97.14± 6.21%) as well as intestine (96.36± 5.87%) was significantly higher for the NISO NE as compared to the plain drug suspension in stomach (16.44± 3.98%) and intestine (12.65± 4.23%). High surface area due to nanosized globules and the lipophilic nature of the formulation enhanced the permeation across the biological membrane.

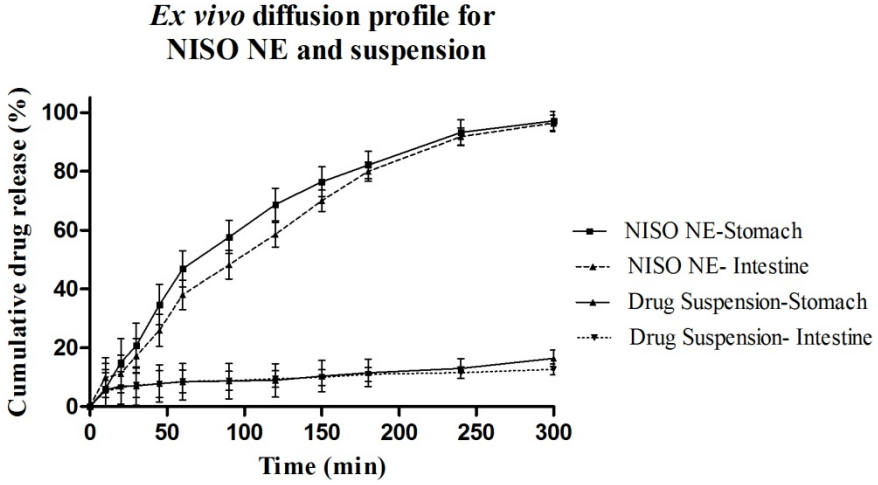

Figure 5.11.20. *Ex vivo* release study of NISO NE and drug suspension from rat stomach and intestine tissue

5.12. Stability study

The optimized formulations of DE NE (Table 5.12.1) and NISO NE (Table 5.12.2) showed negligible changes under the selected storage conditions for parameters in terms of globule size and drug content. Due to small droplet size NE were found stable against creaming or sedimentation. Visual observations also indicated no sign of drug precipitation. The data suggested that the formulation was stable for 6 months at 25 ± 2^0C/60 ± 5% RH condition at room temperature and 40 ± 2^0C/75 ± 5% RH at accelerated conditions.

Table 5.12.1: Results of stability studies for DE NE

Time (months)	Long term study (25 ± 2°C/60% ± 5% RH)		
	Physical Description	**Globule size (nm)**	**Drug content (%)**
Initial	Clear liquid with bluish tint	71.65 ± 1.02	98.04 ± 2.57
1 month	Clear liquid with slight bluish tint	75.54 ± 1.54	98.11 ± 2.87
3 months	Clear liquid with slight bluish tint	74.11 ± 1.11	97.47 ± 2.71
6 months	Clear liquid with slight bluish tint	73.32 ± 1.43	98.68 ± 2.64
	Accelerated Study (40 ± 2°C/75% ± 5% RH)		
1 month	Clear liquid with slight bluish tint	76.04 ± 2.32	98.48 ± 2.93
2 months	Clear liquid with slight bluish tint	72.84 ± 1.32	96.82 ± 2.23
3 months	Clear liquid with slight bluish tint	73.71 ± 1.78	98.66 ± 2.18
6 months	Clear liquid with slight bluish tint	74.29 ± 2.01	98.59 ± 2.54

Table 5.12.2: Results of stability studies for NISO NE

	Long term study (25 ± 2°C/60% ± 5% RH)		
Time (months)	**Physical Description**	**Globule size (nm)**	**Drug content (%)**
Initial	Yellow clear liquid	62.35 ± 2.55	98.87± 2.12
1 month	Yellow clear liquid	65.46± 2.21	97.54± 1.89
3 months	Yellow clear liquid	63.93± 2.32	97.25± 1.55
6 months	Yellow clear liquid	62.23± 2.64	98.12± 1.63
	Accelerated Study (40 ± 2°C/75% ± 5% RH)		
1 Month	Yellow clear liquid	63.71 ± 1.98	98.51± 1.39
2 months	Yellow clear liquid	63.27± 2.53	98.76± 1.99
3 months	Yellow clear liquid	66.34 ± 2.47	98.36± 1.43
6 months	Yellow clear liquid	68.15 ± 2.32	97.75± 2.72

References

1. S.Y. Tang, S. Manickam, T.K. Wei, and B. Nashiru, Formulation development and optimization of a novel Cremophore EL-based nanoemulsion using ultrasound cavitation. Ultrasonics Sonochemistry, 2012. 19(2): p. 330-345.
2. B.J. Aungst, Novel formulation strategies for improving oral bioavailability of drugs with poor membrane permeation or presystemic metabolism. Journal of pharmaceutical sciences, 1993. 82(10): p. 979-987.
3. C.C. Chen and G. Wagner, Vitamin E Nanoparticle for Beverage Applications. Chemical Engineering Research and Design, 2004. 82(11): p. 1432-1437.
4. R. Pangeni, S. Sharma, G. Mustafa, J. Ali, and S. Baboota, Vitamin E loaded resveratrol nanoemulsion for brain targeting for the treatment of Parkinson's disease by reducing oxidative stress. Nanotechnology, 2014. 25(48): p. 485102.
5. H.P. Thakkar, A. Khunt, R.D. Dhande, and A.A. Patel, Formulation and evaluation of Itraconazole nanoemulsion for enhanced oral bioavailability. Journal of microencapsulation, 2015. 32(6): p. 559-569.
6. A.K. Kushwaha, P.R. Vuddanda, P. Karunanidhi, S.K. Singh, and S. Singh, Development and evaluation of solid lipid nanoparticles of raloxifene hydrochloride for enhanced bioavailability. BioMed research international, 2013. 2013.
7. Y. Yuan, Y. Gao, J. Zhao, and L. Mao, Characterization and stability evaluation of β-carotene nanoemulsions prepared by high pressure homogenization under various emulsifying conditions. Food Research International, 2008. 41(1): p. 61-68.
8. M. Duran-Lobato, A. Enguix-Gonzalez, M. Fernandez-Arevalo, and L. Martan-Banderas, Statistical analysis of solid lipid nanoparticles produced by high-pressure homogenization: a practical prediction approach. Journal of nanoparticle research, 2013. 15(2): p. 1443.
9. D.J. McClements, Edible nanoemulsions: fabrication, properties, and functional performance. Soft Matter, 2011. 7(6): p. 2297-2316.
10. K.K. Sawant, J.K. Varia, and S.S. Dodiya, Cyclosporine a loaded solid lipid nanoparticles: optimization of formulation, process variable and characterization. Current drug delivery, 2008. 5(1): p. 64-69.
11. Y. Singh, J.G. Meher, K. Raval, F.A. Khan, M. Chaurasia, N.K. Jain, and M.K. Chourasia, Nanoemulsion: concepts, development and applications in drug delivery. Journal of Controlled Release, 2017. 252: p. 28-49.
12. A. Nagi, B. Iqbal, S. Kumar, S. Sharma, J. Ali, and S. Baboota, Quality by design based silymarin nanoemulsion for enhancement of oral bioavailability. Journal of Drug Delivery Science and Technology, 2017.
13. E. Harrington, The desirability function. Industrial quality control, 1965. 21(10): p. 494-498.
14. S. Mahdi Jafari, Y. He, and B. Bhandari, Nano-emulsion production by sonication and microfluidization—a comparison. International Journal of Food Properties, 2006. 9(3): p. 475-485.
15. M.H. Shahavi, M. Hosseini, M. Jahanshahi, R.L. Meyer, and G.N. Darzi, Evaluation of critical parameters for preparation of stable clove oil nanoemulsion. Arabian Journal of Chemistry, 2015.
16. S.Y. Tang, P. Shridharan, and M. Sivakumar, Impact of process parameters in the generation of novel aspirin nanoemulsions–comparative studies between ultrasound cavitation and microfluidizer. Ultrasonics sonochemistry, 2013. 20(1): p. 485-497.

17. K.K. Sawant, V.P. Mundada, and V.J. Patel, Development and Optimization of w/o/w Multiple Emulsion of Lisinopril Dihydrate Using Plackett Burman and Box-Behnken Designs. J Nanomed Nanotechnol, 2017. 8(1): p. 422.
18. V. Mundada, M. Patel, and K. Sawant, Submicron Emulsions and Their Applications in Oral Delivery. Critical Reviews™ in Therapeutic Drug Carrier Systems, 2016. 33(3).
19. V. Devarajan and V. Ravichandran, Nanoemulsions: as modified drug delivery tool. International journal of comprehensive pharmacy, 2011. 4(01): p. 1-6.
20. S. Priya, M. Koland, and S. Kumari, Nanoemulsion Components Screening of Quetiapine Fumarate: Effect of Surfactant and Co Surfactant. Asian J Pharm Clin Res, 2015. 8(6): p. 136-40.
21. M.J. Lawrence and G.D. Rees, Microemulsion-based media as novel drug delivery systems. Advanced drug delivery reviews, 2000. 45(1): p. 89-121.
22. J. Siepmann and N. Peppas, Modeling of drug release from delivery systems based on hydroxypropyl methylcellulose (HPMC). Advanced drug delivery reviews, 2012. 64: p. 163-174.